Journal of Geosciences, Osaka City University
Vol. 42, Art. 9, p127-159, March, 1999

An Overview of Petrology of Calc-silicate Granulites from the Trivandrum Block, Southern India

M. SATISH-KUMAR

Department of Biology and Geosciences, Shizuoka University, Ohya, Shizuoka 422-8529, Japan.

Abstract

The southern Indian granulite terrain has been the focal area for studies on the role of fluids in granulite petrogenesis for the past two decades. The present contribution is an overview on the metamorphic evolution of metacarbonate lithologies from the southern part this terrain (Trivandrum Block). Field survey in the granulite terrain of Trivandrum Block (TB) was carried out to identify specific outcrops where calc-silicate rocks and marbles are exposed and detailed studies were carried out on an outcrop scale. Based on mineralogy, the calc-silicate rocks are classified into four types: Type-I, lacking wollastonite and grossular, Type-II, wollastonite bearing but grossular absent, Type-III, wollastonite and grossular bearing, and Type-IV, calcite-rich marbles. Detailed petrographic studies reveal a variety of reaction textures overprinting the polygonal, granoblastic, peak-metamorphic assemblages in these rocks. The type-II assemblages provide CO_2 activity estimates of > 0.5 with a peak metamorphic temperature of about 790°C. Initial cooling followed by later CO_2 influx can be deduced from reaction modeling in these calc-silicate rocks. Type-III assemblages are characterized by internal fluid buffering during the peak metamorphism. The reaction topologies produced are good approximations for the peak as well as retrograde mineral assemblages and reaction textures. The textural features interpreted with activity-corrected grids indicate a phase of isobaric cooling from about 835°C to 750°C at 6 kbar. The Type-IV marble assemblages indicate internal fluid buffering followed by localized CO_2 influx. Forsterite+spinel-bearing assemblages were formed under granulite-facies P-T conditions and internal fluid buffering. Phlogopite, pargasite and humite group minerals occur as equilibrium peak mineral assemblages and have high fluorine contents, which attest to the stability of these minerals at granulite facies P-T conditions. Although humite-bearing assemblages suggest low a_{CO_2} for the metamorphic fluid, forsterite + spinel-bearing assemblages reflect moderate to high a_{CO_2} and the local wollastonite + scapolite + grossular-bearing zones were formed under moderate to low a_{CO_2}. Retrograde reaction textures such as scapolite-quartz symplectites after feldspars and calcite, and coronal replacement of dolomite+diopside or tremolite+dolomite after calcte+forsterite or calcite+clinohumite are indicative of retrogression under higher a_{CO_2} conditions. The retrograde metamorphic P-T-fluid evolution of the Trivandrum Block has been revised using the reaction textures in calc-silicate rocks and marbles. The reaction textures now preserved are consistent with post-peak cooling to 750°C whilst pressures were still >5 kbar. This near-isobaric P-T trajectory contrasts with the decompressional (ITD) P-T evolution documented in previous studies of the TB. However, as the previously deduced ITD evolution occurred at temperatures < 750°C, the P-T record in the calc-silicates can be reconciled with that seen in the metapelites if the cooling textures pre-date the ITD. In this scenario, the TB P-T path would be one that initially involved near-isobaric cooling (IBC) at 5-6 kbar from peak conditions of > 830°C to ca. 750°C and subsequently involved continued cooling, but with substantial exhumation, resulting in a final phase of post-peak decompression to 3-4 kbar at temperatures less than 750°C. The ITD phase of this post-peak evolution correlates with medium- to low-pressure fluid infiltration events. This study is unique in the finding of unequivocal evidences of high temperature metamorphism in TB granulites with internal fluid buffering, with an early retrograde cooling event and local fluid infiltration events during later decompression. The results of peak metamorphic conditions and the early cooling event contrasts with the earlier studies in the terrain and are comparable with those observed in other granulite terrains in the East Gondwana ensemble, while some of the textures resulting from carbonic fluid infiltration event are peculiar for the TB.

Key words: Calc-silicate rocks, Reaction textures, Trivandrum Block, Isobaric cooling, Fluid infiltration

Introduction

The petrogenesis of granulite facies rocks has been a topic of frontline research in recent years, since their P-T-t evolutionary history is fundamental to the formulation of geodynamic models for the evolution of the continental crust. Recently, calc-silicate rocks have been shown to provide important constraints on the P-T-t path and fluid history of high-grade terrains (Warren et al., 1987; Motoyoshi et al., 1991; Harley and Buick, 1992; Dasgupta, 1993; Harley et al., 1994; Fitzsimons and Harley, 1994). Wollastonite+scapolite bearing calc-silicate rocks preserve a variety of reactions and tex-

tures which are extremely useful for evaluating peak as well as retrograde P-T-fluid histories (e.g. Harley and Buick, 1992). For example, wollastonite-scapolite bearing calc-silicate assemblages may preserve textures which indicate either isobaric cooling (e.g. grossular + quartz symplectites after wollastonite and plagioclase), isothermal decompression (e.g. scapolite or plagioclase and wollastonite symplectite after grossular and quartz), or the infiltration of fluids (e.g. scapolite + quartz symplectites after wollastonite and feldspar).

Previous studies on granulites of southern India have generally observed the absence of wollastonite-bearing granulites (Ravindrakumar and Venkatesh Raghavan, 1992). However, Harley and Santosh (1995) and Satish-Kumar et al. (1995) have reported wollastonite-bearing calc-silicate rocks from the Kerala Khondalite Belt (KKB), a supracrustal terrain in the southern India. Most of the calc-silicate rocks in the KKB lack grossular garnet and are associated with anhydrous orthopyroxene-bearing assemblages. Satish-Kumar and Harley (1998) observed unique reactions and textures in a grossular-bearing calc-silicate occurrence in the terrain and re-evaluated the metamorphic conditions using activity-corrected mineral equilibrium calculations. These results suggest that calc-silicate granulites are of considerable interest for this terrain, since previous models of the KKB suggest that incipient charnockite formation in the terrain involved an influx of CO_2 (e.g. Santosh et al., 1991, 1993). In this contribution a review on the metamorphic characteristics of the calc-silicate rocks and marbles from the Trivandrum Block is attempted. The fluid conditions and metamorphic evolution of the terrain is also re-evaluated in the light of the new observations.

Regional geology

The Precambrian shield of Peninsular India is a typical Archaean shield, comprising a cratonic nucleus encompassed

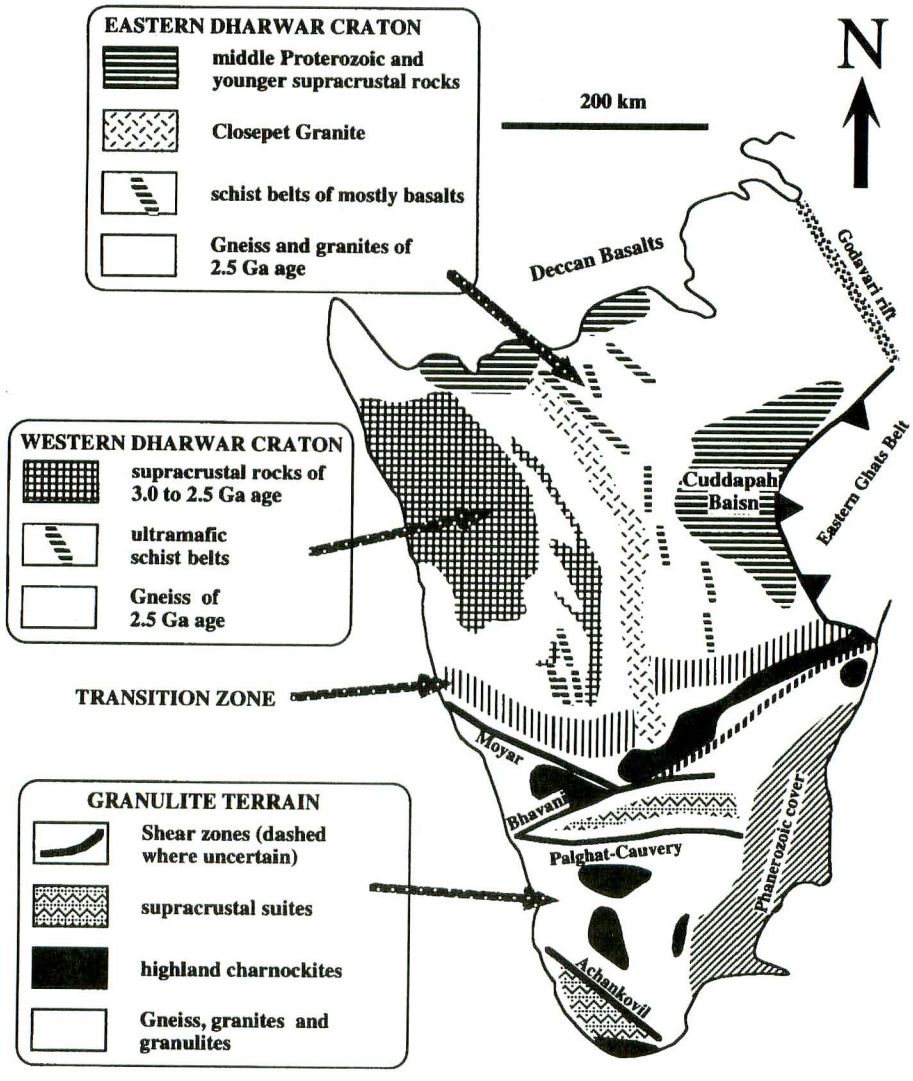

Fig. 1. Regional geological framework of southern peninsular India (after Rogers and Mauldin, 1994).

by mobile belts. The shield is exposed towards the south of the extensive Deccan basalt province in Peninsular India. It consists of the granite-greenstone dominated Dharwar craton in the north, a granulite terrain in the south separated from the craton by a transition zone and the Eastern Ghats mobile belt separated from the craton by a thrust fault (Fig. 1). A concise outline of the regional geology of the shield is discussed below with more emphasis on the southernmost granulite terrain of the Trivandrum Block, which is thematically important in this work.

The Dharwar Craton comprises mainly Archaean tonalitic-trondjemitic-granodioritic (TTG) gneisses (ca. 3.3 Ga; Beckinsale et al., 1980) with overlying volcano-sedimentary supracrustals (ca. 3 Ga; Taylor et al., 1984) and intruded by post tectonic granites (e.g. Clospet granite; 2.5 Ga; Taylor et al., 1984). Traditionally, the craton is divided in to the western and eastern Dharwars by the Closepet granite. The Craton has undergone varying degrees of metamorphism, with a regional gradation from greenschist facies in the north to amphibolite and incipient granulite facies in the south (Rogers, 1986). Metamorphism has been dated as contemporaneous with post tectonic magmatism at around 2.5 Ga (Chadwick et al., 1996; Jayananda et al., 1995). The southern part of the Dharwar Craton consists of a transition zone (Fig. 1) to the higher grade southern granulite terrain, with metamorphic grade increasing from amphibolite facies in the north to granulite facies in the south (Hansen et al., 1995). The transition zone shows no structural, geophysical, or other tectonic discontinuity.

The high grade southern granulite terrain is transected by a network of shear zones of late Proterozoic age (Drury and Holt, 1980; Drury et al., 1984), which have been the basis of delineating the terrain into four major blocks; the Nilgiri Block, the Madras Block, the Madurai Block and the Trivandrum Block (Harris et al., 1994). The major shear zones are the Moyar Shear Zone (between the transition zone and Nilgiri Block), Moyar-Bhavani and Palghat-Cauvery Shear Zones (between Madras/Nilgiri Blocks and the Madurai Block) and the Achankovil Shear Zone between the Madurai Block and the Trivandrum Block. Most of the lineaments are associated with alkaline magmatic activity represented by a suite of alkali granite and syenite plutons (see Rajesh et al., 1996, for a complete review) contemporaneous with the Pan-African activities widely reported in other parts of the Gondwanan fragments, indicating a phase of reactivation of the Shear Zones during the Pan-African.

Recent Nd model age mapping in the southern Indian granulite terrain has identified the Palghat-Cauvery Shear Zone as a major crustal divide between older Archaean granulite crust in the north and the younger supracrustal dominated crust in the south. (Harris et al., 1994, 1996; Brandon and Meen, 1995). The Nilgiri Block and Madras Block are predominantly orthogneiss dominated terrains with acid to intermediate composition consisting primarily of enderbites and charnockites (quartz + plagioclase + K-feldspar + orthopyroxene + garnet ± biotite). Granulite facies metamorphism (750 ± 50°C and 5-9 kbar; Harris et al., 1982; Touret and Hansteen, 1988; Srikantappa et al., 1993) occurred in these terrains at around 2.5 Ga (Peucat et al., 1989; Bernard-Griffiths et al., 1987).

The Madurai Block and Trivandrum Block are dominated by metasedimentary rocks and is separated by the Achankovil Shear Zone. These blocks show abundant evidence of Pan-African tectonothermal activity (Jayananda et al., 1995; Choudhary et al., 1992; Santosh et al., 1992 Bartlett et al., 1995). Recently, high temperature granulite facies metamorphism has been advocated for both the terrains (Raith et al., 1997; Chacko et al., 1996).

The Trivandrum Block (TB)

The region south of the Achankovil Shear Zone, formerly the Kerala Khondalite Belt, is now termed as Trivandrum Block (Fig. 2; Modified after Geological Survey of India, 1995). The Block consists of: (1) the Achankovil metasedimentary rock sequence, which displays Nd model ages of about 1.3 to 1.4 Ga; (2) the Kerala Khondalite Belt which displays Nd model ages between 3.0 and 2.0 Ga; and (3) the Nagarkovil Massif (Bartlett et al., 1995; Bartlett, 1995; Brandon and Meen, 1995; Harris et al., 1996).

The Achankovil metasedimentary sequence occurs within the Achankovil Shear Zone, and in the boundary zone between the Madurai Block in the north and the Kerala Khondalite Belt in the south. The sequence can be considered as a 20km wide zone bounded by two northwest-southeast trending strike-slip shears, the Achankovil shear and the Tenmala shear (Chacko et al., 1987). Kinematic and textural analysis of the rocks in the shear zone indicates primarily a dextral shear sense (Sacks et al., 1997).

The main lithologies of the Achankovil metasedimentary sequence are cordierite-bearing metapelites, calc-silicate rocks and marbles. Cordierite-bearing rocks (cf. Santosh, 1987) occur as elongate patches and show evidence for partial replacement of garnet-bearing assemblages. These rocks yield a well-defined Sm-Nd isochron age of 539 ± 20 Ma (Santosh et al., 1992). The Nd model ages of rocks from this zone (1.3 -1.4 Ga) are typically younger than the surrounding terrains suggesting late Proterozoic crustal addition. Harris et al. (1994) and Brandon and Meen (1995) point out that the younger ages for the Achankovil rocks is a possible reflection of an younger sedimentation age, with source materials being the Vijayan complex of Sri Lanka that has similar ages.

Although most of the Achankovil sequence is characterized by diopside-rich calc-silicate layers, toward the eastern extension of the Achankovil Shear Zone, calcite-rich marble and metapelitic gneiss predominate (Satish-Kumar et al., 1996).

The Kerala Khondalite Belt is a vast metasupracrustal terrain in the southern part of the granulite facies segment of southern India. This belt is bounded on the north by the Achankovil Shear Zone and on the south by the Nagarkovil massif charnockites (Fig. 2). The major rock types in this belt are garnet + biotite ± graphite gneiss, garnet + sillimanite + graphite ± cordierite gneiss and orthopyroxene-bearing granulites. Subordinate lithologies include mafic granulites, quartzite, and calc-silicate rocks. Metamorphism occurred under upper-amphibolite- to granulite-facies P-T conditions. Estimates of peak metamorphic P-T conditions are 750 ± 50 to 850°C and 5 ± 1 kbar (Chacko et al., 1987; Santosh et al., 1993; Chacko et al., 1996; Satish-Kumar et al., 1996). Metapelitic rocks are commonly migmatitic (Braun et al., 1996). A retrograde P-T path dominated by near isothermal decompression has been inferred from the cordierite corona textures and density characteristics of fluid inclusions (Santosh, 1987). Garnet coronas in calc-silicate rocks suggest a retrograde cooling sector in the P-T path prior to the onset of decompression (Satish-Kumar et al., 1996; Satish-Kumar and Harley, 1998).

The KKB forms part of the Proterozoic mobile belt in which sedimentation is thought to have taken place between 3.0 Ga. and 2.0 Ga. Consistent Nd model ages have been obtained for metapelitic rocks and charnockites from different localities in the same terrain (cf. Harris et al., 1994, Brandon and Meen, 1995). A Pan-African tectonothermal event has been widely reported for the terrain, with Santosh et al. (1992) reporting Sm-Nd and Rb-Sr ages from northern part of the KKB, and Choudhary et al. (1992) reporting Pan-African age from a locality near the central KKB. Pan-African ages are also obtained by other geochronological methods such as zircon evaporation (Bartlett et al., 1995). The Pan-African event has been closely linked with the widely reported alkaline magmatism and might have resulted in a terrain-wide thermal rejuvenation (Santosh and Drury, 1988; Santosh et al., 1989; Miller et al., 1995; Rajesh et al., 1996).

The occurrence of numerous examples of charnockite formation in an arrested state with in the garnet-biotite gneisses in KKB have been the focus of several detailed studies on the role of CO_2 in dehydrating the amphibolite-facies gneiss (Srikantappa et al., 1985; Hansen et al., 1987; Santosh et al., 1990,1991; Harris et al., 1993). These models invoke an influx of carbonic fluids through structurally-controlled pathways from lower crustal domains (Santosh et al., 1990,

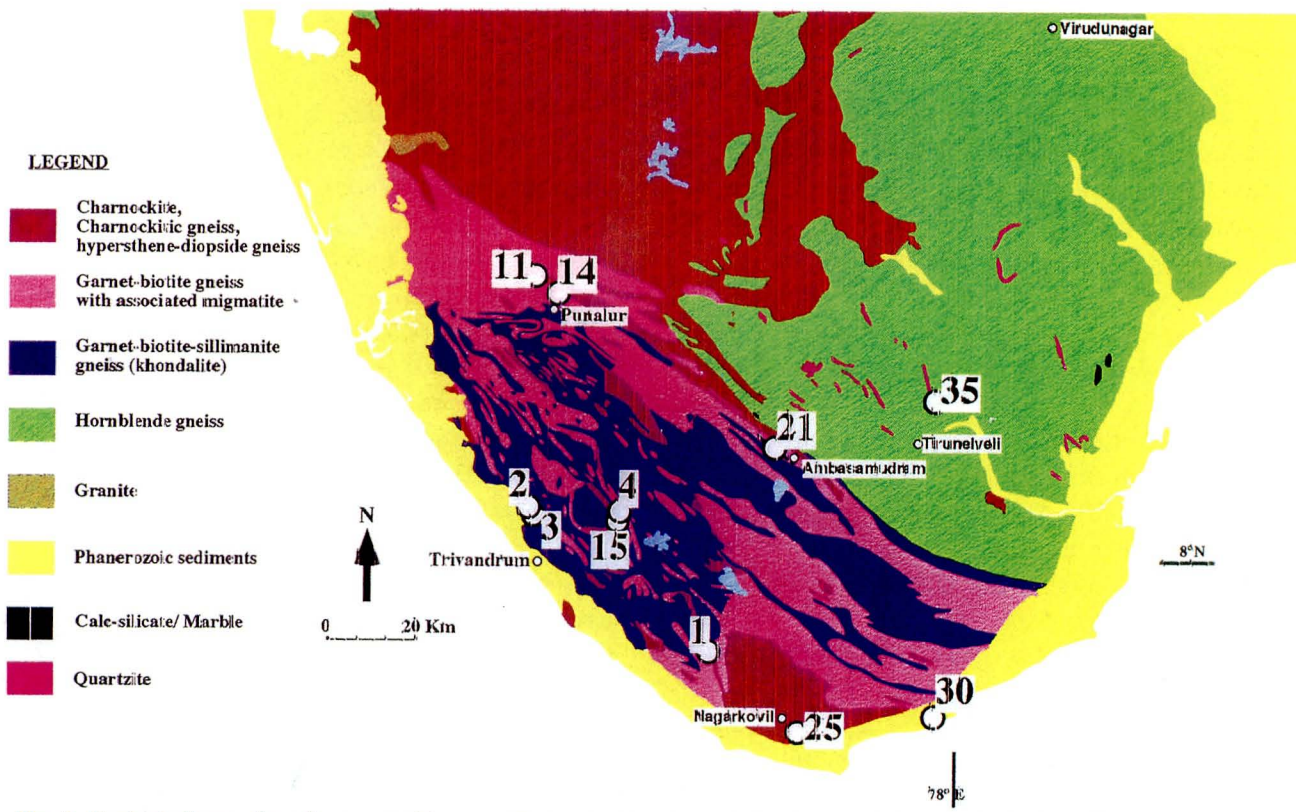

Fig. 2. Geological map of southern part of the granulite terrain of southern India, showing lithological units (modified after Geological survey of India, 1995).

1991; Harris et al., 1993). The orthopyroxene in these patchy charnockites develop by the break down of garnet and biotite in the gneiss (Santosh et al., 1990). Various mechanisms have been invoked by different workers for the movement of carbonic fluids in the lower crust. Farquhar and Chacko (1991) inferred that alkaline dikes carried significant quantities of carbonic fluids, which resulted in the local dehydration of the lithologies. Santosh et al. (1990, 1991) envisaged a structurally controlled fluid movement from lower levels to upper levels in the crust. The precipitation of ^{13}C-enriched graphite in mesoscopic shears has been cited as direct evidence for this (Radhika et al., 1995). Harris and Bickle (1989), from carbon isotopic fronts in close pairs of incipient charnockites and gneiss, envisaged fluid advection across shears and faults, with an ultimate sublithospheric source for CO_2.

The southern tip of Peninsular India consists of a massive charnockite domain popularly known as the Nagarkovil massif. The charnockite in this area are massive and are devoid of garnet and graphite (Santosh, 1996). Evidence for an igneous origin for this massive charnockite comes from the geochemical, oxygen isotopic and melt inclusion studies on the charnockite massif (Santosh, 1996). Also, it can be noticed that at many localities pelitic and calc-silicate xenoliths are present. Sm-Nd mineral isochrons suggest an intrusive age of around 540 Ma for this massif contemporaneous with the regional Pan-African tectonothermal event (Unnikrishnan Warrier et al., 1995).

Field relations

Calc-silicate rocks occur in the southern Indian granulite terrain as unmappable thin bands and lenses interlayered, and mostly concordant with, other rock types. Volumetrically, they are subordinate to other major lithologies such as khondalites, garnet-biotite gneisses and charnockites. Nevertheless, their occurrence and association are important in terms of evaluating the P-T-fluid history of the terrain. Calcite-rich marbles occur as extensive bands and are mappable units. These units are important in deciphering the fluid-rock interaction process.

The calc-silicate rocks/marbles can be generally classified into four types based on their mineralogy: Type-I, calc-silicate rocks lacking wollastonite and grossular-garnet; Type-II, calc-silicate rocks containing wollastonite but lacking grossular; Type-III, wollastonite and grossular bearing calc-silicate rocks; and Type-IV, calcite rich-marbles (Satish-Kumar et al., 1996). Type-I occurs in the Achankovil metasedimentary sequence, Types-II and III commonly occur in the southern part of KKB, around Trivandrum and further south and Type-IV occurs in the Achankovil metasedimentary sequence as well as further north within the Madurai Block (Fig. 2; Table 1). A brief description of the individual calc-silicate / marble localities is given in the following section.

Table 1. Salient features of the calc-silicate rocks and marbles from the Trivandrum Block

Locality No. (cf. Fig. 3.1)	Locality Name	Calc-silicate type	Distribution & dimentions	Associated rock types
1	Nuliyam	Tipe-II	Band 100 × 3m	Charnockite / incipiet charnockite / garnet-biotite gneiss
2	Korani North	type-II	lense 2m × 50cm	Charnockite
3	Korani South	Type-II	Band	Charnockite
25	Arakkakulam	Type-II	Xenolith 25m × 7m	Within massive charnockite
30	Liipuram	Type-II	Band 10m × 5m	Within massive
4	Valiyakalingu	type-III	Band 1km × 100m	Garnet-biotite gneiss
11	Kadakaman	type-I	Lenses and boubins	Chamockite
14	Piravanthur	Type-I	Band 4km × 100m	Charnockite, quartzites, garnet-biotite gneiss
15	Sankaramugham	Type-III	Band 12m × 5m	Garnet-sillimanite gneiss
21	Ambasamudram	Type-IV	Band 10km × 100m	Garent-biotite gneiss, charnockite, quartzites
35	Sankar Nagar	Type-IV	Band 15km × 0.5km	Charnockite, quartzites

Type-I Calc-silicate rocks

The type-I calc-silicate rocks are characterized by an assemblage of diopside + quartz + K-feldspar. They occur in the Achankovil metasedimentary sequence, as boudins less than a meter in dimension or as thin bands in Punalur area. The garnet-biotite gneiss in the vicinity of calc-silicate rock show marked development of augen structures, with post-augen charnockitization being noted in some localities. In a small charnockite quarry inside the Kadakamon (Loc. 11; Fig. 2) Reserve Forest calc-silicate bands and boudins are seen concordant with the compositional layering of the charnockite. Mineralogically the calc-silicate rocks consist mainly of subequal equigranular clinopyroxene and quartz with subordinate amounts of feldspar.

In the Piravanthur area (Loc. 14; Fig. 2), a 50-100 m thick calc-silicate band can be traced for up to 4 km along strike. This band trends in a NW- SE direction, parallel to the Achankovil shear zone, and is intercalated with a number of thin quartzite horizons. These quartzites are sheared and boudinaged parallel to the trend of ACZ. The calc-silicate band is bounded concordantly by charnockites in the northeast and leptynites in the southwest. Structurally, the calc-silicate rock overlies the charnockite. Quartz + clinopyroxene + K-feldspar assemblage occur in subequal proportions.

Type-II Calc-silicate rocks

The type-II calc-silicate rocks are characterized by the occurrence of wollastonite and the absence of grossular. Several such occurrences, some of which are discussed in detail below, have been discovered throughout the southern part of the Kerala Khondalite Belt in the course of this study.

Wollastonite bearing calc-silicate rocks exposed in two locations at Korani (ca. 30 km north of Trivandrum). Both these occurrences are associated with charnockite. The locations, nearly 1000m apart, may represent the strike length of the same band, although their continuity cannot be established in the field. At Korani-north (Loc. 2; Fig. 2) a thin band of calc-silicate occurs in an abandoned charnockite quarry. The thickness of this band is ca. 50 cm. and it can be traced along strike for only about 2 m. It is not clear whether this band is concordant with the adjacent charnockite, since the charnockite is massive and unfoliated, but it is clear that the calc-silicate is concordant with the regional fabric of the khondalites. A graphite-bearing quartz vein cuts across this calc-silicate as well as the charnockite. The charnockite adjacent to calc-silicate is devoid of garnet and biotite, but is graphite bearing. A notable feature of this calc-silicate band is its marked mineralogical zonation, which is defined by a diopside rich marginal zone in contact with the adjacent charnockite, and a wollastonite-rich inner core. The diopside zone is characterized by a granoblastic assemblage of clinopyroxene + scapolite + quartz ± titanite, while the wollastonite zone is characterized by an assemblage of clinopyroxene + wollastonite + scapolite ± titanite.

Calc-silicate rocks are exposed in a location approximately a kilometer south of Korani (Korani-south; Loc. 3; Fig. 2) and occur in the lower horizon of a charnockite quarry. The charnockite is anorthite rich, graphite bearing, and devoid of garnet and biotite. Calc-silicate rocks here show gneissose banding concordant with the regional fabric and defined by modal variations between calcite and silicate phases. The leucocratic, calcite-rich, portion of the calc-silicate band comprises granoblastic calcite + clinopyroxene + scapolite ± titanite. The silicate-rich band consists of an equilibrium assemblage of clinopyroxene + scapolite + wollastonite ± titanite. The silicate-rich band has subequal amounts of clinopyroxene and scapolite whereas calcite and clinopyroxene are the most abundant minerals in the leucocratic band.

A relatively wide band of calc-silicate is exposed at the base of a quarry composed mainly of garnet-biotite gneiss at Nuliyam (Loc. 1; Fig. 2). This locality is described in detail by Jackson and Santosh, 1992; Harley and Santosh, 1995; Satish-Kumar and Santosh, 1998). The gneiss in contact with the calc-silicate is completely charnockitized (Fig. 3a), grading successively into patchy or incipient charnockite and charnockite-free gneiss away from the contact. A biotite-graphite bearing pegmatite (ca. 40 cm. wide) cuts across the lithologies. The flanks of this pegmatite are also charnockitized (Harley and Santosh, 1995). The calc-silicate layer at Nuliyam is concordant with the adjacent gneiss, and has a partially exposed strike length of about 100 m. The thickness of the layer is at least 3 m, but the maximum thickness is unknown (Fig. 3a). Wollastonite-bearing assemblages occur throughout the layer except in the contact zone with charnockite. The mineral assemblages existing in equilibrium in the calc-silicate include wollastonite + scapolite + clinopyroxene + K-feldspar ± graphite ± sulphides with either quartz or calcite. All these minerals occur in coarse polygonal to lobate granoblastic textures, but quartz and calcite are mutually exclusive and only occur together within later localized reaction textures.

A thin band of calc-silicate rock is exposed near Lipuram beach (Loc. 30; Fig. 2), ca. 20 km north of Cape Comorin. This band has a width of more than 5 m and a strike length of about 10m with garnet-biotite gneiss cropping out in the southeast conformably. The banding within the calc-silicate rock defines a general NW-SE trend, dipping 30°NW concordant with the foliation of garnet-biotite gneiss. Mineralogically

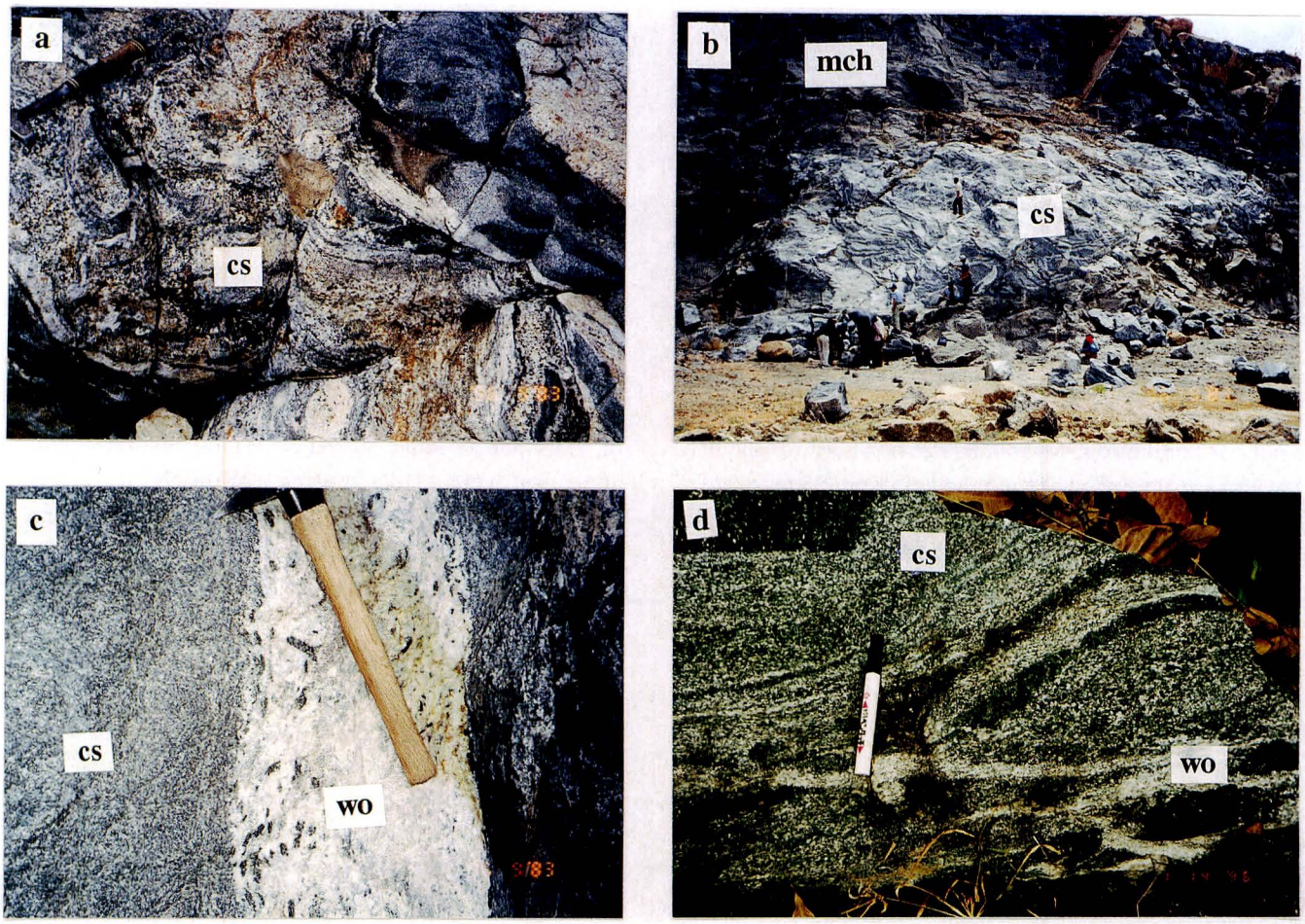

Fig. 3. Field photographs showing typical occurrence of calc-silicate rocks in Trivandrum block.
a. Nuliyam cs: calc-silicate rock, b and c. Arakkakulam mch: massive charnockite, wo: wollastonite vein, d. Vellanad

wollastonite + scapolite + diopside constitute the major minerals with subequal proportions.

Nagarkovil massif comprises of the so-called igneous charnockite pluton emplaced in the southern most part of the southern granulite terrain (Chacko et al., 1996; Santosh, 1996). Towards the contact zone of the charnockite massif with the Kerala Khondalite Belt supracrustals, several pelitic xenoliths can be seen within the charnockite. The Arakkakulam quarry (Loc. 25; Fig. 2), 3 km north of Cape Comorin, comprises massive charnockite with a leucocratic calc-silicate xenolith several meters width (Fig. 3b). The massive charnockite contain orthopyroxene, plagioclase and sulfides and generally lacks garnet. Many wollastonite rich seams and veins can be observed in the calc-silicate xenolith (Fig. 3c). The contact zone between calc-silicate and charnockite is devoid of both wollastonite and orthopyroxene, and has graphite. The leucocratic band (calc-silicate xenolith) in the massive charnockite contains wollastonite, diopside, scapolite, quartz and phlogopite with minor graphite. The calc-silicate rock is generally calcite free, all the calcite appears to have been consumed for the formation of wollastonite and other calc-silicate minerals.

Type-III Calc-silicate rocks

Type-III calc-silicate rocks are characterized by the presence of both wollastonite and grossular. These calc-silicate rocks also occur as bands inter-layered with khondalites and leptynites. Two such occurrences are described below.

An isolated exposure of calc-silicate occurs at Sankaramugham (Loc. 15; Fig. 2) and its contacts with other lithologies are obscured due to lateritization. This particular locality has been studied in detail by Satish-Kumar and Harley (1998). Nearby exposures include massive charnockites and khondalites. The calc-silicate exposure has a width of about 5-m and a strike length of about 12-m. Both medium- and coarse-grained assemblages are present and show gneissose fabrics concordant with the regional foliation. Several thin wollastonite-bearing veins traverse this banding (Fig. 3d). Grossular-bearing calc-silicate horizons occur in the central portion of the band. In grossular absent bands, polygonal textured equilibrium mineral assemblage of wollastonite + scapolite + clinopyroxene + anorthite ± titanite is typical. Grossular bearing layers have a granoblastic textured assemblage of anorthite + scapolite + wollastonite + grossular +

clinopyroxene ± titanite.

An extensive band of calc-silicate can be traced to about 1 km along strike at Valiakalingu (Loc. 4; Fig. 2). The unit has a maximum thickness of about 100-m, and is concordant with the regional trend of the nearby metapelites and associated charnockites. Petrologically this calc-silicate is similar to Sankaramugham calc-silicate rocks.

Type-IV Calcite-rich Marbles

An extensive band of marbles and associated calc-silicate rocks occurs in the northeastern part of Ambasamudram, southern Tamil Nadu. This band can be traced for about 10 km along strike and varies in thickness from 25 m to 300 m (Satish-Kumar and Santosh, 1996c). It is structurally concordant with the adjacent lithologies, which include leptynites charnockitized to different degrees in the vicinity of the calc-silicate band. Intense deformation in the calc-silicate band is shown by boudinage, disruption and rotation of marly layers or bands enclosed within the dominant calcite marble. A later deformation produced mylonites and flaser fabrics, which cut across both marbles and included marly horizons. The marble band is intercalated with quartzite bands of varying thickness and is often graphite bearing. This band consists primarily of calcite-rich marble, including spinel + forsterite and scapolite-bearing assemblages, but the largely disrupted aluminous and quartzite layers (marly bands) or horizons may contain wollastonite and scapolite. A humite + chondrodite + spinel + magnesian calcite assemblage have been reported in a marble from this locality (Krishnanath, 1981). Within the marble itself, most of the variations observed are only between the types and modes of mafic minerals, and almost everywhere calcite/ magnesian calcite comprises more than half of the mineral mode.

Analytical procedures

Mineral assemblages were determined petrographically, and reaction histories were deduced from reaction textures (symplectites and coronas). Some mineral phases which were difficult to identify by optical properties alone (e.g. humite group) were separated by hand picking and X-ray powder diffraction patterns were observed as a confirmation.

Electron microprobe analyses (EPMA) of representative calc-silicate assemblages from the different localities were carried out using a JEOL-JXA 8600MX super probe housed at the University of Kochi, Japan. The analyses were done with an accelerating voltage of 15 kV and a beam diameter of 2-3 μm. Both natural and synthetic standards were used, and oxide ZAF correction was performed throughout. Carbonate minerals were analyzed with an accelerating voltage of 10 kV and a beam diameter of 10 μm. Fluorine, chlorine and sulfur were analyzed using a WDS (JEOL-JXA 733, housed at Tokyo University, Japan) with a probe current of 15 nA and accelerating voltage of 15 kV. The beam diameter was kept as 5 μm. Additional EPMA analyses were obtained using a Cameca Camebax 4 spectrometer microprobe from University of Edinburgh (UK), with an accelerating voltage of 20 kV, beam current 18nA, and diameter of 3-4 μm, and data reduction carried out using an on-line PAP correction procedure. Few quantitative analyses of fluorine for humite minerals were obtained using a JEOL-JXA 8800 housed at the National Institute of Polar Research, Tokyo (Japan). The analytical conditions were accelerating voltage 15 kV, beam current 15nA and minimum beam diameter (1 μm). Bence and Albee (1968) correction was used. Finally, the reproducibility of the analyses was checked with the newly installed Shimadzu EPMA-8705 at Osaka City University (Japan). The analytical conditions were accelerating voltage 15 kV, beam current 4 nA and a beam diameter of 1 μm. Bence and Albee (1968) correction was used.

Peak metamorphic mineral assemblages

Table 2 lists the mineral assemblages observed in the calc-silicate rocks covered as part of the present study.

Table 2. Mineral assemblages in calc-silicate rocks from the Trivandrum Block

Locality	Loc. No.	Type	Wo	Scp	Cpx	Grt	Sph	Cal	Qtz	Gr
Kadakamon	11	I		*	*		*		*	
Piravanthur	14	I			*		*		*	
Korani-north	2	II	*	*	*		*	*		
Korani-south	3	II	*	*	*		*	*		
Nuliyam	1	II	*	*/-	*		*	*/-	*/-	*
Arakkakulam	25	II	*	*	*		*		+	
Lipuram	30	II	*	*	*		*			
Sankaramugham	15	III	*	*	*	*/-	*		*	*
Valiakalingu	4	III	*	*	*	*/-	*		*	

* Porphyroblastic phase; */- porphyroblastic and retrograde phase
Mineral abbreviations are after Kretz(1983)

Type-I calc-silicate rocks

The Type-I calc-silicates are characterized by the granular assemblage of clinopyroxene + quartz + K-feldspar + plagioclase ± titanite ± calcite ± Fe-Ti oxides (Fig. 4a). These rocks have sub-equal amounts of quartz and clinopyroxene. Most of the calcite present is secondary.

Type-II calc-silicate rocks

This type of calc-silicate rocks is characterized by a granoblastic assemblage of wollastonite + scapolite +

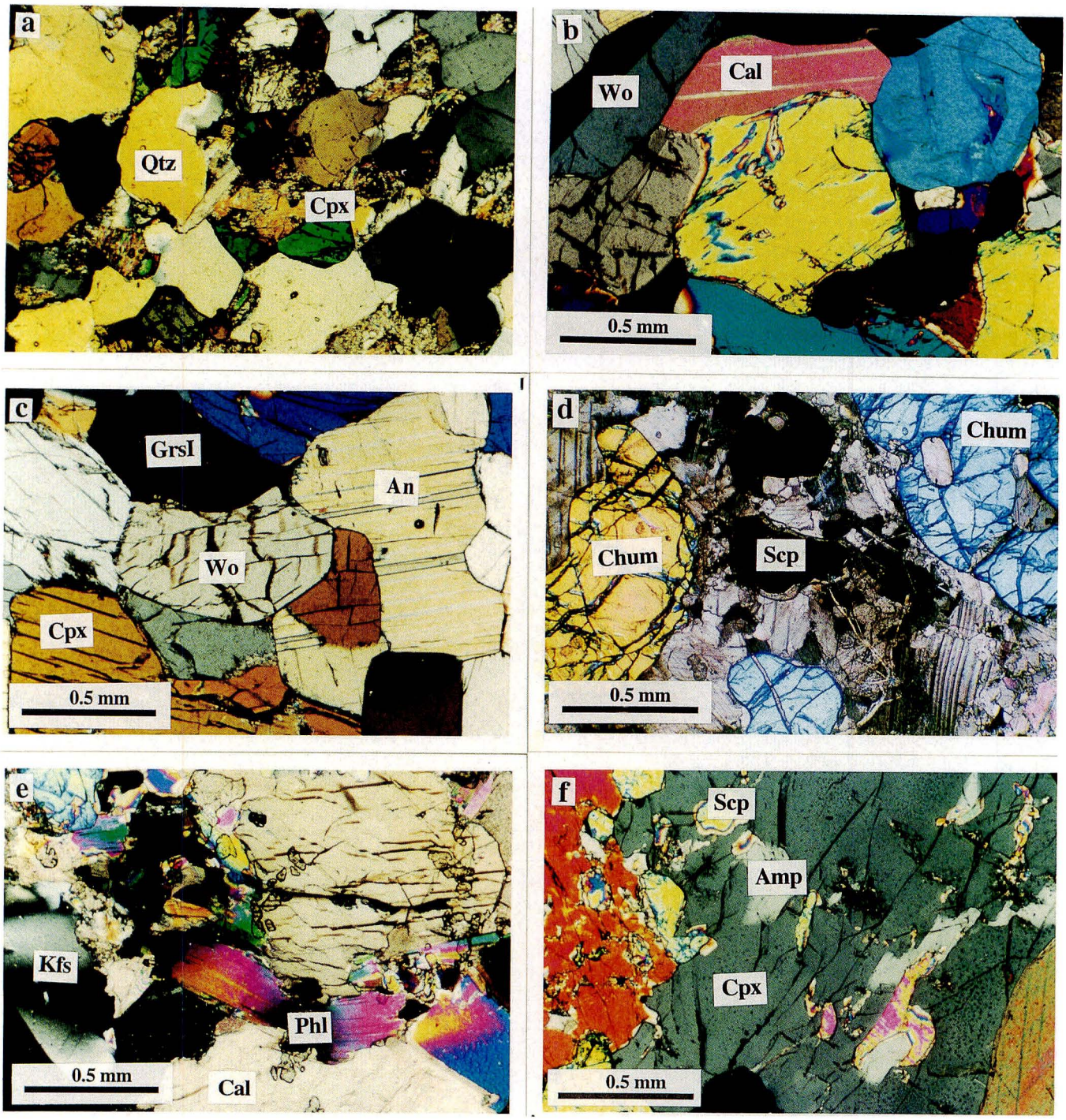

Fig. 4. Photomicrographs showing typical peak metamorphic mineral assemblages in TB calc-silicate rocks. All in crossed nicols. (a) granular Type-I calc-silicate mineral assemblage (b) wollastonite-scapolite-clinopyroxene assemblage in Type-II calc-silicate rocks at Nuliyam (c) granular wollastonite, grossular (GrsI) clinopyroxene and anorthite assemblage in Type-III assemblage (d) clinohumite-spinel-calcite association in Type-IV marbles (e) pargasitic amphibole with surrounding phlogopite and K-feldspar (f) large clinopyroxene crystal with scapolite and amphibole inclusions.

clinopyroxene (Fig. 4b). Polygonal equigranular granoblastic texture is exhibited with well-equilibrated 120° mineral triple-junctions. The three minerals occur in sub-equal modes and the banding is commonly controlled by the difference in the mode of clinopyroxene. The minor phases are feldspars, quartz or calcite, titanite and graphite.

Type-III calc-silicate rocks

The calc-silicate occurrence at Vellanad is zoned or layered, with bands of garnet-bearing (GrsI) calc-silicate occurring in the core of the outcrop (assemblage-A; Fig. 4c) and garnet-absent calc-silicate occurring on the margins (assemblage-B). The fabric-forming minerals in both assemblages A and B are similar, and include wollastonite, scapolite, clinopyroxene, plagioclase (AnI) and titanite. These minerals form an equigranular, polygonal granoblastic texture with layering controlled by modal variations of clinopyroxene. The two peak assemblages can be summarized as follows, thus forming the typical assemblages for type-III calc-silicate rocks.

A: Grs + Wo + Scp + An (+ Cpx + Ttn) (Cal, Qtz)

B: Wo + Scp + An (+ Cpx + Ttn) (Cal, Qtz, Grs)

Type-IV calcite-rich marbles

Most of the assemblage variations in calcite-rich marbles reflect the types and modes of the minor, Mg-rich minerals. More than half of the modal proportion of marble samples consists of calcite or magnesian calcite. The granulite-facies calcite-rich marbles comprises of the following mineral assemblages (Table 3)

(i) calcite + forsterite + spinel ± dolomite ± diopside

(ii) calcite + clinohumite + spinel ± titanite ± graphite (Fig. 4d)

(iii) calcite + clinohumite + spinel + forsterite + phlogopite ± diopside ± tremolite ± titanite ± graphite

(iv) calcite + phlogopite + K-feldspar + titanite ± quartz ± graphite (Fig. 4e)

(v) calcite + diopside + tremolite + phlogopite ± scapolite ± plagioclase ± graphite (Fig. 4f)

(vi) calcite + graphite

These calc-silicate mineral assemblages are set in a granoblastic matrix of calcite.

Retrograde reactions and textures

Reactions and textures developed in calc-silicate rocks/marbles can be assigned to either prograde or retrograde sectors of the metamorphic evolution. Prograde reactions resulted in granoblastic assemblages in all types of calc-silicate rocks/marbles in TB. These granoblastic assemblages have been overprinted by a variety of retrograde reactions that are significant in discussing the pressure-temperature-fluid history of the terrain. The type-I assemblages do not show any retrograde reaction textures.

Type-II calc-silicate rocks

In type-II calc-silicate rocks, polygonal grains of scapolite are seen retrogressed to symplectitic intergrowth of plagioclase and calcite with little quartz (Fig. 5a and b) indicating the vapor absent equilibrium:

scapolite = plagioclase + calcite + quartz R1

Polygonal wollastonite grains are partially replaced (Satish-Kumar et al., 1995) with finer grained calcite + quartz intergrowth (Fig. 5c) implying the reaction,

Table 3. Mineral assemblages in Type-IV marbles from Ambasamudram

Locality	Sample No.	Cal	Dol	Fo	Phl	Spl	Amph	Chu	Gr	Cpx	Scp	Wo	Grt	Fld	Qtz
Uchankulam N	SK6-1	*		*	*	*	*		*		-				
Uchankulam N	SK6-2	*		*	*	*	*		*					*	
Uchankulam N	SK6-4	*	-		*	*	*/-	*	*	*					
Uchankulam S	SK21-1	*	-						*						
Uchankulam S	SK21-13	*	-		*					*	*	*	*	*	*
Uchankulam S	SK21-2b	*				*			*	*					
Uchankulam S	SK21-2a	*		*	*		*		*	-	-				
Uchankulam S	SK21-2aC	*	-		*		*								
Agathiyarpatti	SK20-3	*	-			*			*	*	-				
Agathiyarpatti	SK20-1	*	-		*		*/-		*	*	-			*	
Agathiyarpatti	W 22-3	*	-						*						*
Agathiyarpatti	SK20-5	*	-	*	*	*	*	*	*	-					
Kottavilappatti	SK7-6	*			*		*/-		*						
Kottavilappatti	SK7-11	*	-		*	*	*	*	*	*	-				
Kottavilappatti	SK7-2	*	-	*	*	*		*	*	*					

* Porphyroblastic phase; */- porphyroblastic and retrograde phase

Mineral abbreviations are after Kretz(1983)

wollastonite + CO_2 = calcite + quartz R2

In some of the localities, clinopyroxene is retrogressed to form amphibole (Fig. 5d) representing the reaction,

clinopyroxene + H_2O + CO_2 =

amphibole + calcite + quartz R3

Meionite + quartz symplectites (Fig. 5e and f) developed on wollastonite and calcite + quartz pseudomorphs after wollastonite reacting with K-feldspar are often observed in these calc-silicate rocks. This indicates the metasomatic reaction (cf. Harley and Santosh, 1995):

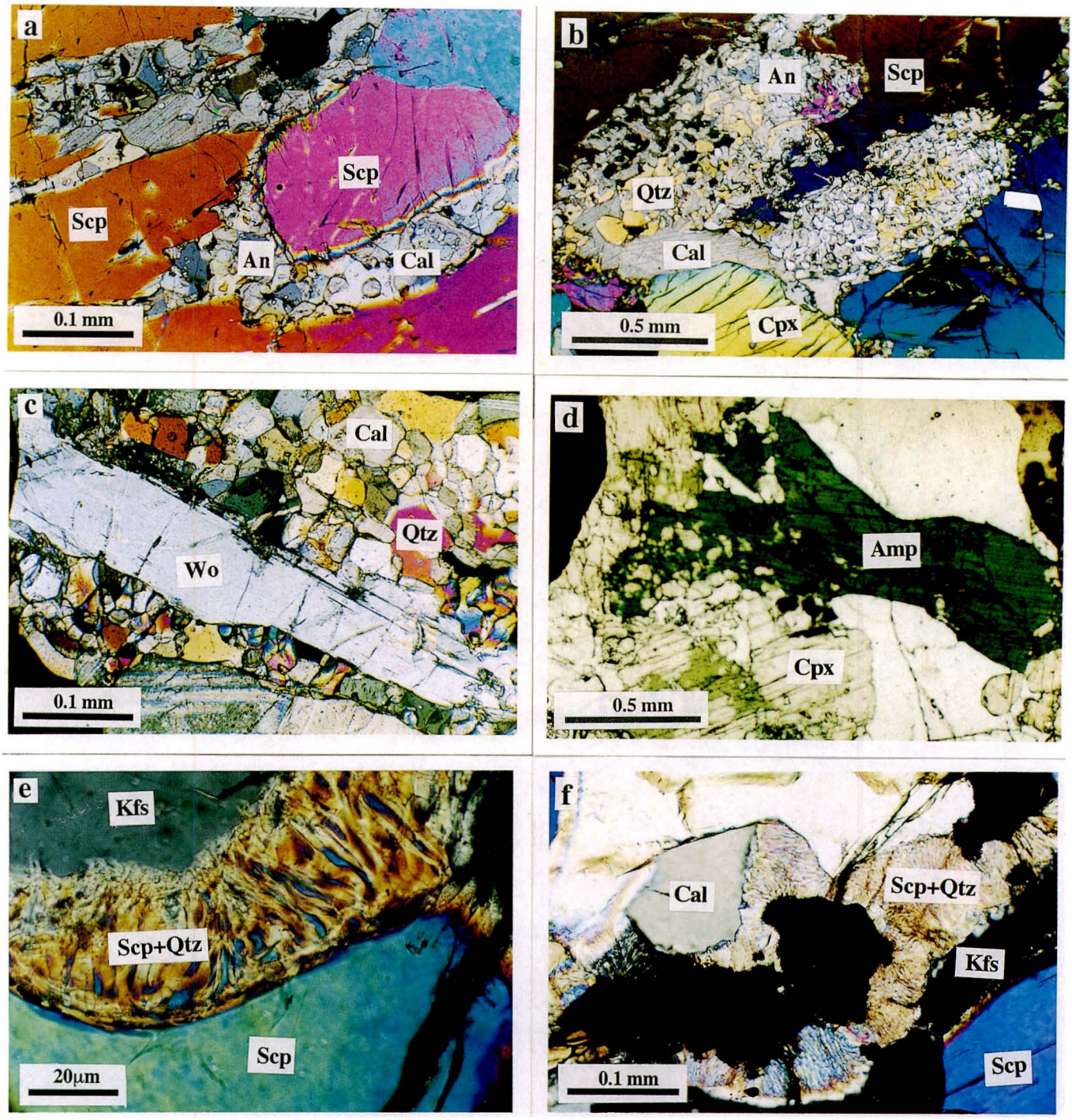

Fig. 5. Photomicrographs showing retrograde reaction textures in Type-II calc-silicate assemblages; (a) scapolite retrogressing to form coronal anorthite + calcite quartz at Korani locality (b) scapolite retrogressing to form coronal anorthite + calcite quartz at Nuliyam locality (c) wollastonite breaking down to form granular calcite + quartz at Nuliyam (d) retrograde amphibole formation at the expense of clinopyroxene at Korani (e, f) Scapolite-quartz symplectites forming after k-feldspar and calcite + quartz after wollastonite at Nuliyam. This texture has been the key in deducing the fluid infiltration model at Nuliyam. Note the fining of the symplectite near k-feldspar indicating it as the dominant phase in reaction progress.

Wollastonite + K-feldspar + Na^+ (fluid)
= scapolite + quartz + K^+ (fluid) R4

At Nuliyam locality the contact zone assemblage between wollastonite-bearing calc-silicate rock and orthopyroxene bearing charnockite is characterized by feldspar + quartz + clinopyroxene, set in a granular mosaic with minor amounts of calcite and titanite. Most of the K-feldspars are rimmed by myrmekitic intergrowth of plagioclase + quartz. The plagioclase + quartz intergrowth become more fine towards the contact with K-feldspar. Quartz forms fine cuspate blebs with less than 10 microns to about 50 microns width. Away from K-feldspar, the quartz blebs coalesce to form larger

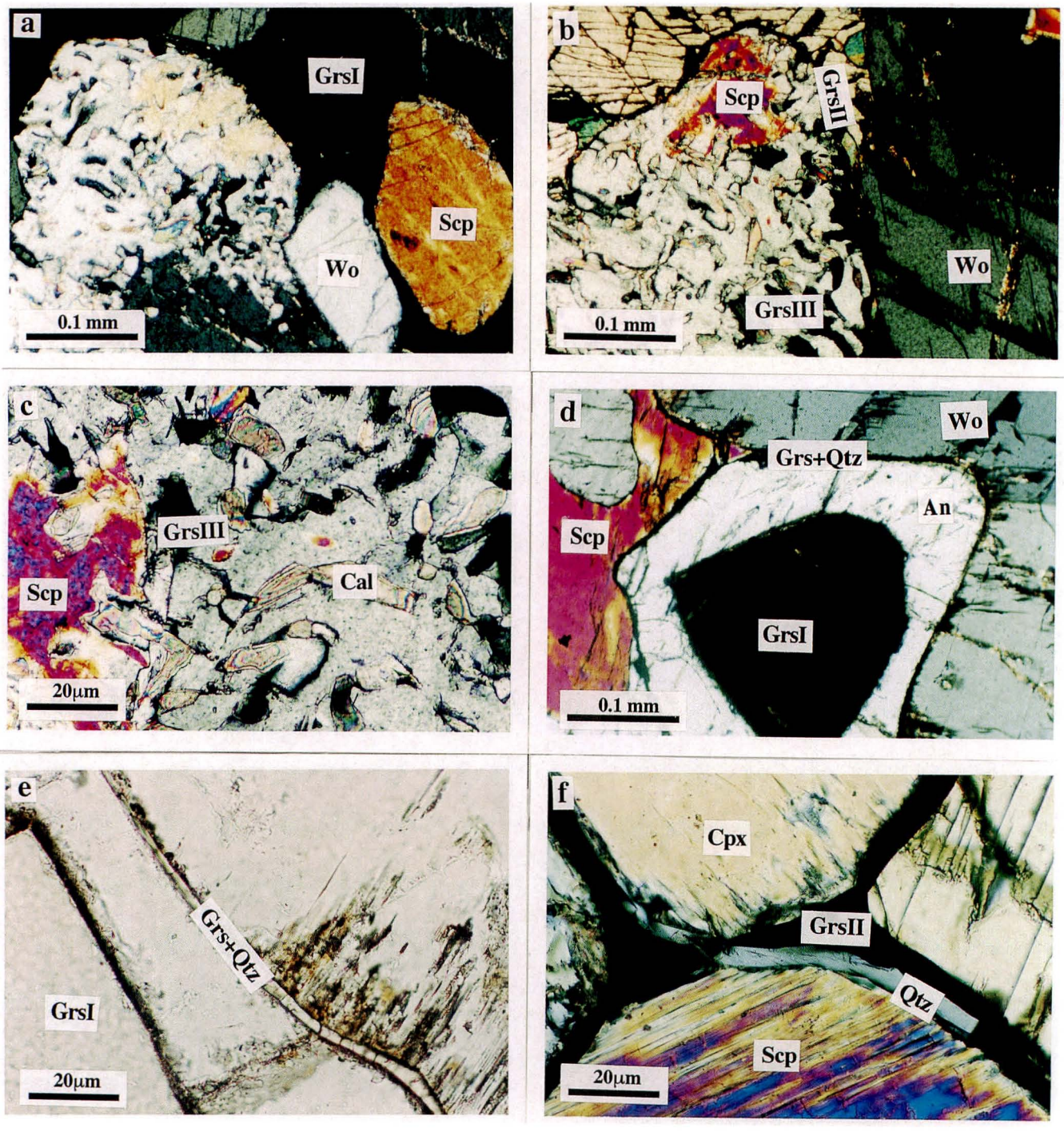

Fig. 6. Photomicrographs showing typical scapolite break down reaction in type-III calc-silicate rocks at Vellanad: (a) scapolite breaking down to anorthite and calcite, crossed nicols (b) grossular (GrsII) rims between earlier plagioclase and wollastonite, crossed nicols (c) formation of grossular (GrsIII) after anorthite calcite and quartz (d) earlier grossular (GrsI) inclusion in plagioclase, crossed nicols (e) grossular (GrsII) + quartz corona between plagioclase and wollastonite, open nicols (f) grossular + quartz corona between scapolite and clinopyroxene, crossed nicols.

grains. The plagioclase in the intergrowth is optically continuous.

Symplectitic intergrowth of this type can be seen in several places in the examined sample, and in most cases the plagioclase is untwinned.

Type-III calc-silicate rocks

The well-equilibrated granoblastic texture is overprinted by several later reaction textures that are either localized to individual grains or grain clusters or restricted to grain boundaries. These include scapolite grains replaced partially to wholly by symplectitic intergrowth of plagioclase (AnII) and calcite with minor quartz. This texture is observed both in assemblage A and B (Fig. 6a and b) and is ascribed to the reaction R1

Garnet coronas occur between wollastonite and plagioclase + calcite pseudomorphs after scapolite in assemblage B (Fig. 6b) indicating the equilibrium:

wollastonite + plagioclase + calcite = garnet + CO_2 .....(R5)

Garnet (GrsIII) blebs (Fig. 6c) form within the plagioclase (AnII) + calcite + quartz pseudomorphs after scapolite in assemblage B. This corresponds to the reaction:

plagioclase + calcite + quartz = garnet + CO_2 .....(R6)

Garnet (GrsII) + quartz coronas occur between wollastonite and plagioclase in assemblage B (Fig. 6d and e), suggesting the reaction:

wollastonite + plagioclase = garnet + quartz .....(R7)

Garnet coronas also occur on contacts of scapolite, wollastonite or plagioclase with clinopyroxene (Fig. 6f). With the involvement of clinopyroxene the reacting system becomes multivariant as FeO and MgO have to be considered along with the Na_2O-CaO-Al_2O_3-SiO_2-vapor system (e.g. Harley et al., 1994). Generally the garnet-forming reactions involving clinopyroxene can be explained using one among the following multivariant equilibria

clinopyroxene + scapolite(ss) + wollastonite + calcite = garnet(ss) + CO_2 .....(R8)

clinopyroxene + scapolite(ss) + wollastonite = garnet(ss) + quartz + CO_2 .....(R9)

clinopyroxene + scapolite(ss) + wollastonite + calcite = garnet(ss) + quartz + CO_2 .....(R10)

clinopyroxene + wollastonite + plagioclase = garnet(ss) + quartz .....(R11)

as discussed by several authors (Warren et al., 1987; Harley et al., 1994; Fitzsimons and Harley, 1994).

Type-IV calcite-rich marbles

The calcite-rich marble shows retrograde reaction textures that overprint the peak metamorphic assemblages. Forsterite typically is rimmed by fine inter growths of dolomite and diopside, probably suggesting the reaction:

forsterite + calcite + CO_2 = dolomite + diopside .....(R12)

Calcite and anorthite grain boundaries show coronal growth of meionite (Fig. 7a), suggesting the reverse reaction of R1. Scapolite-quartz symplectites (Fig. 7b) are developed between calcite and feldspars following the metasomatic equilibrium R3 described earlier.

Forsterite and calcite grains have reacted to form tremolite and dolomite:

forsterite + calcite + CO_2 + H_2O + HF = tremolite + dolomite .....(R13)

Exsolution of calcite is present in sample SK 21 1; the exsolved phase having higher Mg-content.

Clinohumite and chondrodite typically show coronas of amphibole + carbonate minerals (Fig. 7c, d and e), suggesting the following reactions:

F-clinohumite + calcite + CO_2 = F-tremolite + dolomite + H_2O .....(R14)

F-clinohumite + diopside + H_2O + CO_2 = F-tremolite + calcite .....(R15)

Grossular bearing rocks

Grossular-bearing rocks within the marble are feldspar and calcite rich, and also contain clinopyroxene, scapolite and titanite. The coexistence of grossular-rich garnet + calcite + quartz, with garnet having wollastonite and scapolite inclusions (Fig. 7f) suggest the vapor absent reaction:

wollastonite + scapolite = grossular + calcite + quartz .....(R16)

Grossular + quartz also occur in textural equilibrium with wollastonite + scapolite suggesting the reaction R7.

Aluminous quartzite layers

Numerous disrupted layers of aluminous quartzite occur in the marble band. High variance mineral reaction zones are present between clinopyroxene + anorthite + scapolite-bearing assemblages of the aluminous quartzite and the host marble. The aluminous quartzite consists predominantly of quartz + feldspar, with subordinate opaque minerals. Little calcite is present. The reaction zones typically contain wollastonite + scapolite + clinopyroxene + titanite + calcite. The formation of reaction rinds around marls indicates a simple bimetasomatism that resulted from chemical potential gradi-

ents in SiO_2, CaO and Al_2O_3. Gradients in μSiO_2 and μAl_2O_3 were evidently significant, because a typical sequence of reaction zone is An+Scp+Qtz(aluminous quartzite) Scp+Qtz Scp+Wol Scp+ Cc Cc(marble).

While scapolite and wollastonite in the reaction zones might have formed through the forward reactions of R1 and R2, diopside and titanite can be products of the following reactions

dolomite + quartz = diopside + CO_2 .....(R17)

calcite + rutile + quartz = titanite + CO_2 .....(R18)

Also these reaction zones exhibit the retrogression of scapolite to plagioclase and calcite via reaction R1.

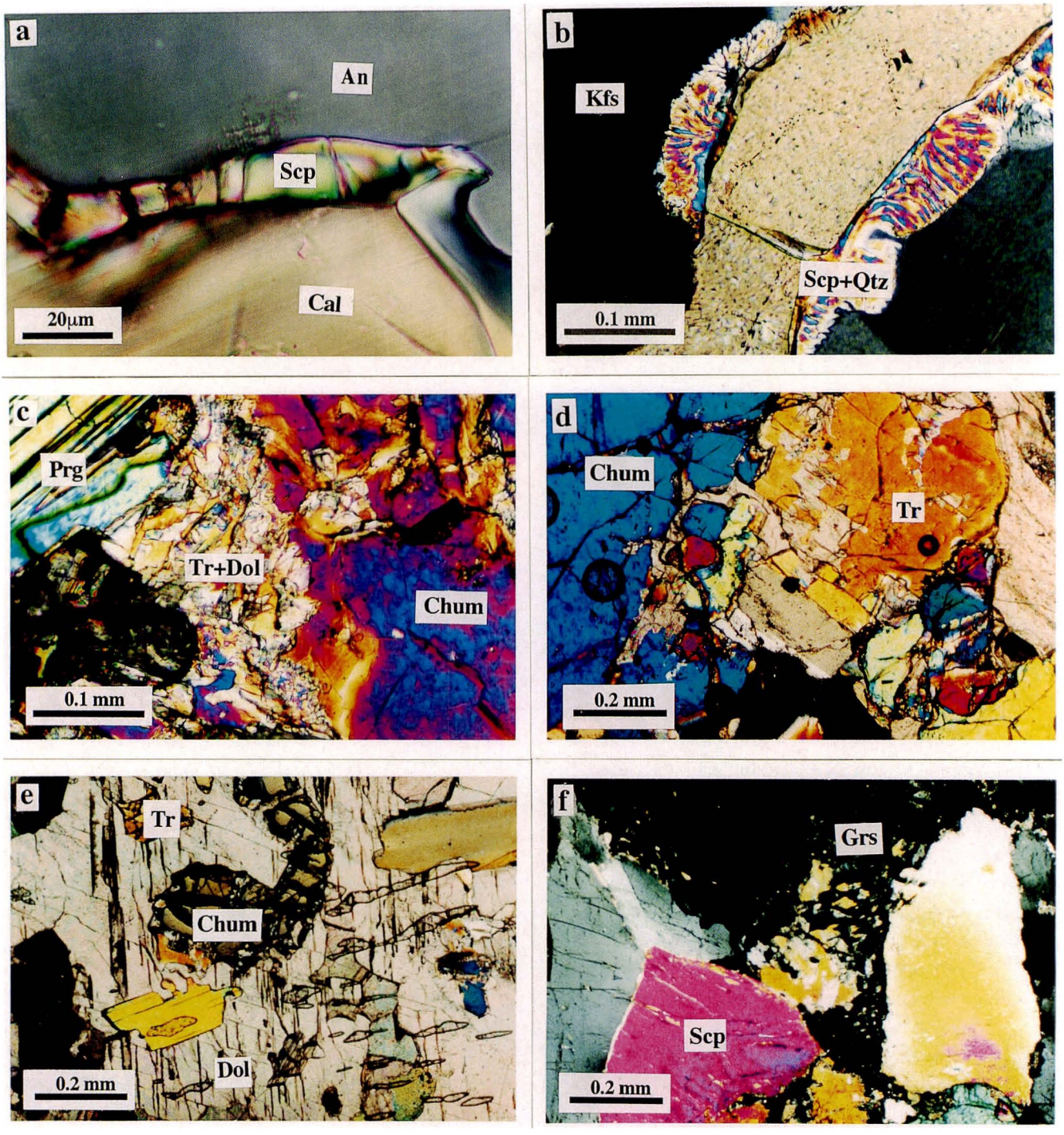

Fig. 7. Retrograde reaction textures observed in Type-IV marbles at Ambasamudram all photomicrographs in crossed nicols (a) Formation of scapolite rim between feldspar and calcite (b) Scapolite-quartz symplectites forming after K-feldspar and calcite +quartz after wollastonite (a) forsterite retrogressing to form diopside and dolomite (c) clinohumite retrogressing to form dolomite and tremolite (d) clinohumite retrogressing to form dolomite and tremolite (e) relict clinohumite in tremolite + phlogopite + dolomite matrix (f) grossular forming after scapolite and wollastonite

Table 4. Mineral chemistry of garnet from calc-silicate rocks

Analysis No.	15 5C 1	15 5C 2	15 5C 8	15 5C 9	15 5C 15	15 5C 16	15 5C 20	21 1 61	21 1 62	21 1 63
Position/type	Grs-I	Grs-I	Grs-II	Grs-II	Grs-III	Rim:Grs-I	Core Grs-I	core	rim	core
SiO_2	38.86	39.00	39.08	39.31	39.39	38.95	38.87	39.26	39.82	39.20
TiO_2	0.48	0.51	0.38	0.43	0.17	0.55	0.49	0.00	0.00	0.09
Al_2O_3	19.57	19.42	19.71	19.57	19.75	19.23	19.94	18.58	19.13	17.91
Cr_2O_3	0.12	0.02	0.00	0.00	0.00	0.07	0.00	0.00	0.00	0.00
Fe_2O_3*	2.98	3.29	4.15	3.42	3.22	3.49	3.93	5.46	4.63	5.67
FeO	4.25	4.64	3.91	4.49	3.87	4.57	3.81	0.72	1.77	1.45
MnO	0.56	0.68	0.69	0.66	0.70	0.65	0.20	0.34	0.45	0.36
MgO	0.24	0.25	0.18	0.21	0.07	0.20	0.70	0.04	0.02	0.03
CaO	32.44	32.25	32.90	32.65	33.12	32.40	32.50	33.75	35.33	35.19
Na_2O	0.02	0.00	0.01	0.01	0.03	0.00	0.00	0.00	0.02	0.00
Total	99.52	100.05	101.00	100.75	100.31	100.11	100.42	100.16	101.18	99.90
Cations on the basis of 12 oxygen atoms										
Si	2.995	2.996	2.975	2.998	3.011	2.994	2.964	3.005	3.015	3.018
Ti	0.028	0.030	0.022	0.025	0.010	0.032	0.028	0.000	0.000	0.005
Al	1.778	1.758	1.768	1.759	1.779	1.742	1.792	1.676	1.708	1.625
Cr	0.007	0.001	0.000	0.000	0.000	0.004	0.000	0.000	0.000	0.000
Fe^{3+}	0.173	0.190	0.238	0.196	0.185	0.202	0.226	0.314	0.264	0.328
Fe^{2+}	0.274	0.298	0.249	0.286	0.247	0.294	0.243	0.046	0.112	0.093
Mn	0.037	0.045	0.045	0.043	0.046	0.042	0.013	0.022	0.029	0.024
Mg	0.028	0.028	0.020	0.024	0.008	0.023	0.079	0.005	0.002	0.004
Ca	2.679	2.655	2.683	2.668	2.712	2.667	2.655	2.931	2.866	2.903
Na	0.002	0.000	0.001	0.001	0.004	0.000	0.000	0.000	0.002	0.000
Total	8.001	8.001	8.001	8.000	8.002	8.000	8.000	7.999	7.998	8.000
X_{Mg}	0.09	0.09	0.07	0.08	0.03	0.07	0.25	0.10	0.02	0.04
X_{Alm}	0.091	0.098	0.083	0.095	0.082	0.097	0.081	0.015	0.037	0.031
X_{Py}	0.012	0.015	0.015	0.014	0.015	0.014	0.004	0.007	0.010	0.008
X_{Spss}	0.009	0.009	0.007	0.008	0.003	0.008	0.026	0.002	0.001	0.001
X_{Grs}	0.797	0.781	0.790	0.785	0.811	0.778	0.792	0.822	0.825	0.797

* calculated

Quartzites and quartz veins

The marble layer is interlayered with nearly monomineralic quartzite, some of which contain graphite. A few later quartz-rich veins also cut the marble. In general the contacts between veins and the marble are sharp and reaction zones are absent. These features suggest that P-T and/or the fluid conditions were outside the stability limits for new calc-silicate minerals.

Mineral Chemistry

Garnet (Table 4)

Garnet occurs as both porphyroblasts and coronal rims in type-III assemblages and locally in type-IV assemblages. All garnets are typically grandite in composition with low pyralspite contents. Porphyroblastic garnets rarely show zonation, whereas grossular component increases marginally in coronal garnets. Three textural types of garnet occur in assemblage A: granoblastic GrsI, coronal GrsII and blebby GrsIII. Chemically all these garnets are grandite-rich with little pyralspite content (2-5 mol%). The granoblastic garnets show only minor core to rim compositional variation. The grossular content of coronal garnets are similar to those of the granoblastic garnets, both averaging 78 mol% Grs. GrsIII garnet blebs formed after plagioclase + calcite + quartz pseudomorphs have higher grossular contents (82 mol% Grs)(Fig. 8). Garnet in type-IV dolomitic marbles is typically more grossular rich than in type-III assemblages.

Clinopyroxene (Table 5)

Clinopyroxene is a diopside-hedenbergite solid solution. The X_{Mg} for type-I calc-silicate clinopyroxene clusters around 0.65, but for other type calc-silicate rocks it varies considerably from location to location. At Korani, a type-II calc-silicate locality, the clinopyroxene has an average X_{Mg} of 0.25, while Nuliyam clinopyroxene have an average of 0.55. Clinopyroxene from of Type-III calc-silicates has a X_{Mg} range of 0.35-0.40. CaTs contents are low (2-5 mol%), and esseneite

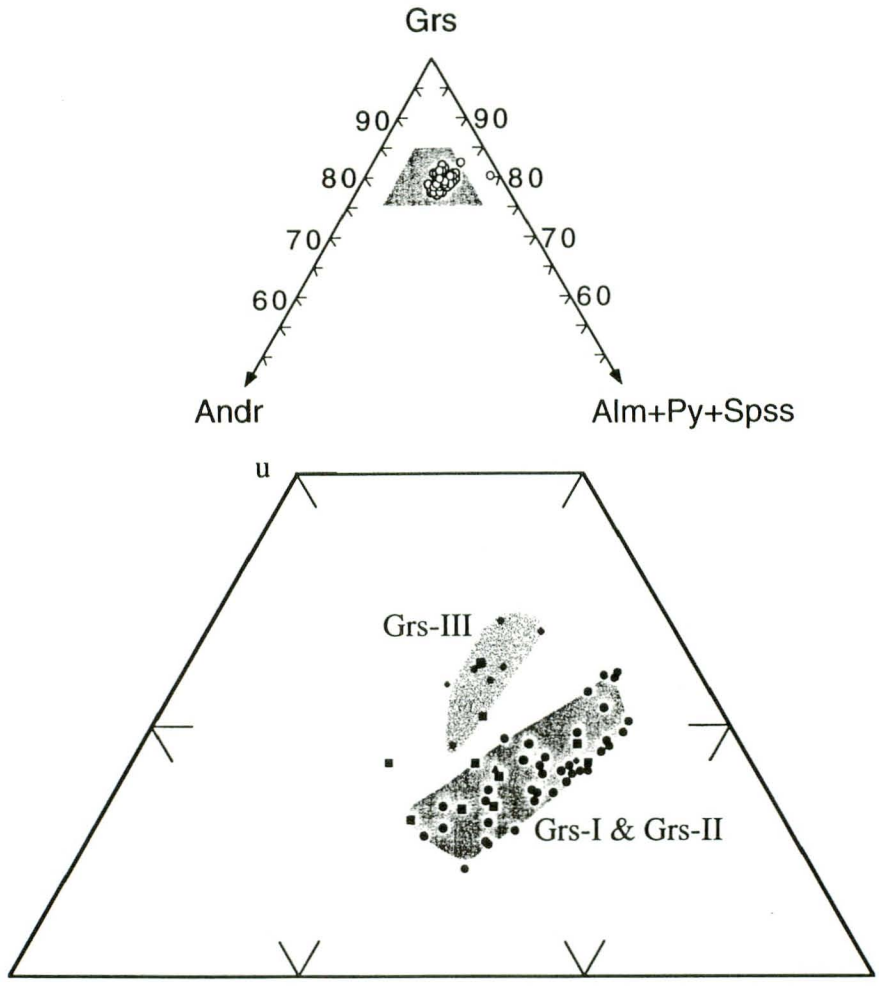

Fig. 8. Compositional variation of different generations of garnet at a Type-III locality (after Satish-Kumar and Harley, 1998)

Table 5. Mineral chemistry of clinopyroxene and wollastonite from calc-silicate rocks and marbles

Sample No.	SK1-1B		SK15-3		SK21-1		SK1-1B		SK15-3	
Analysis No.	cpx 2-	cpx 6-1	cpx 8-8	cpx 1 1B	cpx 4-18A	cpx 5-19B	wol 3-5B	wol 4-6A	wol 7-8B	wol 7-8C
SiO_2	51.32	51.65	49.27	46.59	53.95	53.13	52.05	52.03	51.21	51.31
TiO_2	0.07	0.03	0.05	0.14	0.05	0.04	0.00	0.01	0.00	0.00
Al_2O_3	0.90	0.94	0.82	1.27	0.91	0.97	0.00	0.03	0.02	0.00
Cr_2O_3	0.03	0.06	0.00	0.03	0.00	0.03	0.00	0.00	0.02	0.03
Fe_2O_3*	0.21	1.26	0.40	0.00	0.00	1.29	0.00	0.00	0.82	0.64
FeO	13.25	13.12	18.85	19.10	9.33	8.13	0.94	0.93	0.00	0.00
MnO	0.09	0.06	0.78	0.64	0.22	0.20	0.08	0.08	0.39	0.35
MgO	8.99	9.24	4.70	4.82	12.15	12.22	0.07	0.08	0.01	0.01
CaO	24.35	24.56	23.98	23.70	24.64	24.84	47.35	46.76	47.85	47.63
Na_2O	0.19	0.15	0.05	0.09	0.26	0.34	0.05	0.04	0.02	0.01
K_2O	0.00	0.00	0.00	0.00	0.00	0.00	0.00	0.00	0.00	0.00
Total	99.39	101.05	98.89	99.38	101.52	101.20	100.53	99.97	100.33	99.98
Cations on the basis of 6 oxygen atoms										
Si	1.981	1.965	1.975	1.973	1.994	1.972	2.004	2.011	1.982	1.990
Ti	0.002	0.001	0.001	0.004	0.001	0.001	0.000	0.000	0.000	0.000
Al	0.041	0.042	0.039	0.059	0.040	0.043	0.000	0.001	0.001	0.000
Cr	0.001	0.002	0.000	0.001	0.000	0.001	0.000	0.000	0.001	0.001
Fe^{3+}	0.006	0.036	0.012	0.000	0.000	0.036	0.000	0.000	0.024	0.019
Fe^{2+}	0.428	0.418	0.631	0.635	0.288	0.252	0.030	0.030	0.000	0.000
Mn	0.003	0.002	0.027	0.022	0.007	0.007	0.003	0.002	0.013	0.012
Mg	0.517	0.523	0.281	0.286	0.670	0.676	0.004	0.005	0.000	0.001
Ca	1.007	1.001	1.030	1.010	0.976	0.988	1.953	1.936	1.984	1.979
Na	0.014	0.011	0.004	0.007	0.019	0.024	0.004	0.003	0.001	0.000
K	0.000	0.000	0.000	0.000	0.000	0.000	0.000	0.000	.0.000	0.000
Total	4.000	4.001	4.000	3.997	3.994	4.000	3.998	3.989	4.006	4.001
X_{Mg}	0.55	0.56	0.31	0.31	0.70	0.73				

* calculated

Table 6. Mineral chemistry of scapolite from calc-silicate rocks and marbles

Analysis No.	SK1-1B 4-3A	4-4A	4-7A	SK15-3 4-5c	5-6a	5-6b	SK21-1 1-1	3-1	3-1	3-1
SiO_2	45.63	45.53	45.17	43.28	43.05	42.53	46.48	47.22	46.91	46.58
TiO_2	0.01	0.00	0.00	0.03	0.00	0.03	0.00	0.00	0.00	0.00
Al_2O_3	27.54	27.81	27.65	28.73	28.85	28.58	27.26	27.35	27.37	27.36
FeO	0.47	0.50	0.40	0.57	0.56	0.55	0.13	0.20	0.17	0.19
MnO	0.01	0.00	0.00	0.00	0.02	0.00	0.00	0.00	0.02	0.00
MgO	0.09	0.12	0.08	0.06	0.05	0.06	0.04	0.05	0.07	0.04
CaO	19.31	19.85	19.66	21.49	21.71	21.78	18.51	18.49	18.63	18.34
Na_2O	1.67	1.85	1.89	1.39	1.33	1.25	3.11	3.09	2.95	3.14
K_2O	0.59	0.63	0.65	0.15	0.12	0.14	0.15	0.16	0.18	0.17
Total	98.31	96.28	96.50	95.71	95.70	94.91	95.68	96.56	96.30	95.81
Cations on the basis of 25 oxygen atoms										
Si	6.991	6.929	6.929	6.662	6.632	6.612	7.074	7.114	7.090	7.077
Ti	0.001	0.000	0.000	0.004	0.000	0.003	0.000	0.000	0.000	0.000
Al	4.973	4.988	4.998	5.211	5.237	5.237	4.890	4.856	4.875	4.899
Fe	0.061	0.064	0.052	0.074	0.072	0.071	0.016	0.025	0.021	0.024
Mn	0.001	0.000	0.000	0.000	0.003	0.000	0.000	0.000	0.003	0.000
Mg	0.022	0.027	0.018	0.013	0.011	0.014	0.008	0.012	0.017	0.0010
Ca	3.169	3.236	3.231	3.544	3.584	3.628	3.018	2.984	3.016	2.986
Na	0.495	0.545	0.561	0.416	0.397	0.375	0.919	0.902	0.864	0.926
K	0.115	0.122	0.127	0.029	0.024	0.028	0.029	0.031	0.035	0.032
Total	15.827	15.910	15.917	15.951	15.960	15.969	15.955	15.925	15.921	15.953
Cations on the basis of Si+Al=12										
Si	7.012	6.977	6.971	6.733	6.705	6.696	7.095	7.131	7.111	7.091
Ti	0.001	0.000	0.000	0.004	0.000	0.003	0.000	0.000	0.000	0.000
Al	4.988	5.023	5.029	5.267	5.295	5.304	4.905	4.869	4.889	4.909
Fe	0.061	0.064	0.052	0.075	0.073	0.072	0.016	0.025	0.021	0.024
Mn	0.001	0.000	0.000	0.000	0.003	0.000	0.000	0.000	0.003	0.000
Mg	0.022	0.026	0.018	0.013	0.011	0.014	0.008	0.012	0.017	0.010
Ca	3.179	3.259	3.251	3.582	3.624	3.675	3.027	2.992	3.025	2.992
Na	0.497	0.549	0.564	0.420	0.402	0.381	0.921	0.905	0.866	0.927
K	0.115	0.123	0.128	0.029	0.025	0.029	0.029	0.030	0.035	0.032
Total	15.875	16.021	16.013	16.124	13.137	16.173	16.002	15.964	15.967	15.985
%Meionite	84	83	82	89	89	90	76	76	77	76
Eq.An.	66.30	67.40	67.60	75.57	75.61	76.80	63.49	62.28	62.98	63.63

component ($CaFe^{3+}AlSiO_6$), calculated from Fe^{3+} as determined using charge balance constraints on 4 cation formula-unit pyroxene analyses, is also < 2 mol%. Type-IV calcite-rich marbles have clinopyroxene with an X_{Mg} of 0.71, which is the highest in the TB calc-silicate rocks. The clinopyroxene of the type-I calc-silicate rocks have comparatively higher Al_2O_3 contents than other types.

Wollastonite (Table 5)

Wollastonite is almost pure and usually contains only minor amounts of FeO and MnO.

Scapolite (Table 6)

Scapolite is commonly reported in terms of EqAn, which is calculated from analyses normalized with Si+Al equal to 12 cations (Shaw, 1960; Evans et al., 1969). Even though there is not much regional variation in the KKB scapolite, those from type-III assemblages have an apparently higher EqAn content of around 76. Scapolite show different compositions in assemblages A and B. Equivalent anorthite (EqAn) values of scapolite from assemblage A is around 86 while that of assemblage B is around 76. The EqAn content of other calc-silicate locations lie in the range of 62 to 68. These EqAn values are similar to those of a large population of scapolite summarized by Moecher and Essene (1991), and to those reported from Nuliyam by Harley and Santosh (1995), but are generally lower than those of scapolite from higher-temperature granulites equilibrated at 800°C or greater (Warren et al., 1987; Motoyoshi et al., 1991; Harley and Buick, 1992; Harley et al., 1994). Scapolite have XCO_3 $\{CO_3/(CO_3+Cl+SO_4)\}$ ratios near unity, except for one sample from Nuliyam calc-silicate rock which has considerable Cl content.

Feldspars (Table 7)

Both primary and secondary feldspars are present in KKB calc-silicate rocks. The X_{An} content of plagioclase in type-I calc-silicate rocks is around 0.4 whereas it is almost pure anorthite in other calc-silicate rocks, except for the calc-silicate - charnockite contact zone at Nuliyam. In Type-III calc-silicates the anorthite content in plagioclase varies slightly between different generations. X_{An} of the granoblastic plagioclase in assemblage A is around 0.98, whereas that of ret-

Table 7. Mineral chemistry of plagioclase from calc-silicate rocks and marbles

Sample No.	SK 1-10C		SK 14-0		SK 15-3		SK 3-3A	
Analysis No.	plg 4-7B	plg 6-8A	plg 2-4	plg 2-5	plg 2-12B	plg 2-12C	plg 2-10B	plg 4-11
SiO_2	70.77	53.92	57.81	59.09	43.32	42.85	44.18	43.71
TiO_2	0.01	0.04	0.00	0.01	0.00	0.01	0.00	0.00
Al_2O_3	21.51	26.94	27.26	26.86	35.52	35.50	34.90	34.94
FeO	0.23	0.16	0.18	0.17	0.07	0.20	0.14	0.02
MnO	0.00	0.02	0.00	0.02	0.08	0.02	0.00	0.00
MgO	0.00	0.00	0.01	0.03	0.00	0.03	0.01	0.01
CaO	1.19	10.43	7.77	8.55	19.67	19.89	19.01	19.33
Na_2O	10.09	5.36	5.96	6.35	0.34	0.33	0.63	0.63
K_2O	0.07	0.21	0.98	0.21	0.01	0.02	0.02	0.02
Total	103.87	97.06	99.96	101.29	99.02	98.84	98.89	98.66
Cations on the basis of 8 oxygen atoms								
Si	2.966	2.505	2.588	2.607	2.027	2.012	2.064	2.050
Ti	0.000	0.001	0.000	0.000	0.000	0.000	0.000	0.000
Al	1.062	1.475	1.438	1.397	1.959	1.964	1.922	1.931
Fe	0.008	0.005	0.007	0.006	0.003	0.007	0.005	0.001
Mn	0.000	0.001	0.000	0.001	0.003	0.001	0.000	0.000
Mg	0.000	0.000	0.000	0.002	0.000	0.002	0.000	0.001
Ca	0.053	0.519	0.373	0.404	0.986	1.000	0.952	0.971
Na	0.820	0.483	0.517	0.543	0.031	0.030	0.058	0.058
K	0.004	0.012	0.056	0.012	0.001	0.001	0.001	0.001
Total	4.914	5.001	4.979	4.972	5.008	5.018	5.002	5.013
X_{An}	0.06	0.51	0.39	0.42	0.97	0.97	0.94	0.94
X_{Ab}	0.94	0.48	0.55	0.57	0.03	0.03	0.06	0.06
X_{Kfs}	0.00	0.01	0.06	0.01	0.00	0.00	0.00	0.00

Table 8. Mineral chemistry of phlogopite from Ambasamudram marbles

Sample No.	Sk 7 11				Sk 7 2				
Analysis No.	18phl	19phl	20phl	21phl	45phl	51phl	52phl	63phl	64phl
SiO_2	41.06	41.59	41.28	42.28	41.98	41.81	41.86	41.85	40.66
TiO_2	0.25	0.22	0.26	0.21	0.22	0.18	0.17	0.20	0.16
Al_2O_3	14.17	13.89	14.24	13.49	14.06	13.58	12.30	13.91	13.38
Cr_2O_3	0.04	0.02	0.00	0.00	0.00	0.00	0.00	0.00	0.00
FeO	0.70	0.69	0.78	0.70	0.43	0.42	0.52	0.38	0.46
MnO	0.05	0.00	0.00	0.08	0.01	0.00	0.04	0.00	0.00
MgO	26.88	27.05	26.76	27.22	26.30	26.62	27.25	26.35	26.30
CaO	0.02	0.01	0.01	0.02	0.03	0.06	0.09	0.02	0.05
Na_2O	0.68	0.76	0.74	0.73	0.57	0.59	0.51	0.55	0.53
K_2O	9.03	9.20	9.07	9.38	9.18	9.51	9.04	9.52	9.58
P_2O_5	0.00	0.02	0.00	0.00	0.00	0.01	0.00	0.00	0.00
NiO	0.00	0.03	0.03	0.18	0.00	0.00	0.00	0.05	0.06
V_2O_3	0.00	0.00	0.00	0.00	0.04	0.00	0.04	0.06	0.00
Cl	0.01	0.03	0.05	0.04	0.04	0.05	0.04	0.04	0.06
.=O	0.00	-0.01	-0.01	-0.01	-0.01	-0.01	-0.01	-0.01	-0.01
F	3.68	3.70	3.23	2.96	2.51	2.82	2.88	2.70	2.04
.=O	-1.55	-1.56	-1.36	-1.24	-1.06	-1.19	-1.21	-1.14	-0.86
SO_3	0.00	0.06	0.01	0.02	0.00	0.05	0.00	0.03	0.00
Total	95.01	95.69	95.09	96.02	94.29	94.49	93.52	94.50	92.39
Si	5.839	5.881	5.852	5.938	5.952	85.949	6.013	5.948	5.906
Ti	0.027	0.024	0.028	0.022	0.023	0.019	0.018	0.021	0.018
Al	2.375	2.315	2.380	2.233	2.351	2.277	2.083	2.330	2.291
Cr	0.004	0.002	0.000	0.000	0.000	0.000	0.000	0.000	0.000
Fe	0.083	0.081	0.093	0.082	0.051	0.050	0.062	0.046	0.055
Mn	0.006	0.000	0.000	0.009	0.001	0.000	0.005	0.000	0.000
Mg	5.695	5.700	5.654	5.698	5.558	5.645	5.832	5.581	5.692
Ca	0.003	0.001	0.001	0.002	0.004	0.009	0.014	0.002	0.007
Na	0.094	0.104	0.102	0.099	0.078	0.081	0.072	0.076	0.074
K	0.819	0.830	0.820	0.840	0.830	0.863	0.828	0.863	0.887
Total	14.945	14.937	14.930	14.924	14.849	14.893	14.927	14.866	14.931
X_{Mg}	0.99	0.99	0.98	0.99	0.99	0.99	0.99	0.99	0.99

Table 9. Mineral chemistry of amphibole from Ambasamudram marbles

Sample No.	SK7 11				Sk7 2			
Analysis No.	2amph2	5amph	6amph	7amph	53amph	54amph	55amph	56amph
SiO_2	43.10	43.11	42.99	43.13	42.74	42.63	43.53	44.04
TiO_2	0.17	0.21	0.12	0.18	0.31	0.38	0.44	0.46
Al_2O_2	15.59	15.97	15.89	15.58	14.62	14.44	15.15	15.14
Cr_2O_2	0.03	0.06	0.02	0.05	0.00	0.00	0.00	0.03
Fe_2O_3*	0.45	0.82	1.26	1.08	0.56	0.30	0.00	0.00
FeO	0.86	0.47	0.00	0.10	0.27	0.42	0.57	0.56
MnO	0.05	0.07	0.03	0.00	0.00	0.00	0.05	0.01
MgO	19.02	18.99	19.38	19.44	19.62	19.65	19.36	19.49
CaO	13.50	13.42	13.36	13.60	13.64	13.66	13.47	13.56
Na_2O	2.21	2.17	2.15	2.05	2.31	2.36	2.45	2.44
K_2O	1.35	1.43	1.49	1.54	1.02	0.97	0.96	0.95
F	1.80	1.68	2.04	1.74	1.53	1.88	1.57	1.53
Cl	0.06	0.06	0.08	0.07	0.09	0.04	0.09	0.06
H_2O*	1.23	1.30	1.12	1.27	1.33	1.17	1.34	1.38
O=F,Cl	0.77	0.72	0.88	0.75	0.67	0.80	0.68	0.66
Total	98.64	99.03	99.05	99.08	97.37	97.10	98.29	98.97
Si	6.152	6.124	6.105	6.126	6.167	6.171	6.207	6.230
Al^{iv}	1.848	1.876	1.895	1.874	1.833	1.829	1.793	1.770
Al^{vi}	0.775	0.797	0.764	0.733	0.653	0.634	0.753	0.753
Ti	0.018	0.022	0.013	0.020	0.034	0.041	0.047	0.049
Cr	0.003	0.007	0.002	0.006	0.000	0.000	0.000	0.004
Fe^{3+}	0.049	0.088	0.135	0.115	0.061	0.032	0.000	0.000
Fe^{2+}	0.103	0.056	0.000	0.012	0.032	0.051	0.068	0.067
Mn	0.006	0.009	0.004	0.000	0.000	0.000	0.006	0.001
Mg	4.047	4.020	4.103	4.115	4.221	4.241	4.115	4.111
Ca	2.064	2.042	2.032	2.069	2.109	2.119	2.058	2.055
Na	0.611	0.597	0.593	0.564	0.645	0.664	0.678	0.668
K	0.246	0.258	0.269	0.278	0.188	0.179	0.174	0.171
F	0.814	0.753	0.915	0.783	0.700	0.861	0.707	0.685
Cl	0.015	0.015	0.020	0.017	0.021	0.009	0.021	0.014
OH*	1.171	1.232	1.065	1.200	1.279	1.130	1.272	1.302
Total	17.922	17.897	17.915	17.912	17.943	17.961	17.900	17.878
Amph. group	Ca	Ca	Ca	Ca	Ca	Ca	Ca	Ca
(Ca+Na)(B)	2.06	2.04	2.03	2.07	2.11	2.12	2.06	2.05
Na (B)	0.00	0.00	0.00	0.00	0.00	0.00	0.00	0.00
(Na+K)(A)	0.86	0.86	0.86	0.84	0.83	0.84	0.85	0.84
$Mg/(Mg+Fe^2)$	0.98	0.99	1.00	1.00	0.99	0.99	0.98	0.98
$Fe^3/(Fe^3+Al^{vi})$	0.06	0.10	0.15	0.14	0.09	0.05	0.00	0.00
Sum of S2	13.00	13.00	13.02	13.00	13.00	13.00	12.99	12.98
X_F	0.41	0.38	0.46	0.39	0.35	0.43	0.35	0.34
Amph. names	pargasite	pargastite	potassian-pargasite	potassian-pargasite	potassian-pargasite	pargasite	pargasite	pargasite

* calculated

rogressed plagioclase after scapolite is 0.99. The X_{An} of plagioclase in garnet-absent assemblages is 0.97. K-feldspar that is present in some locations has only low Na content.

Titanite

Titanite occurs as an accessory mineral in all locations and has a high content of minor and REE elements.

The Type-IV calcite-rich marbles have low dolomite content (less than 2 modal %) and silicate minerals have high Mg:Fe ratios.

Forsterite

Subhedral to rounded grains of forsterite (X_{Mg} = 0.98) occurs in a calcite rich matrix in marbles.

Spinel

Magnesian rich spinel is typical for the marbles (X_{Mg} 0.85-0.90). These spinels have about 2 wt. % zinc.

Phlogopite (Table 8)

Phlogopite is almost pure magnesium end member (Phl98 Ann2). It has high fluorine content (2.5 to 3.8 wt%) and low titanium content.

Amphibole (Table 9)

Polygonal pargasitic amphibole is the most dominant

Table 10. Mineral chemistry of clinohumite from calc-silicate rocks and marbles

Analysis No.	7/11-2hum	7/11-14hum	7/11-15hum	7/2-46hum	7/2-47hum	7/2-48hum	7/2-49hum	7/2-50hum	7/2-68hum	7/2-69hum
SiO_2	34.67	34.48	34.66	36.92	37.94	36.98	38.05	37.56	36.11	36.21
TiO_2	0.39	0.31	0.33	0.37	0.14	0.48	0.37	0.41	0.41	0.58
Al_2O_3	0.01	0.00	0.01	0.00	0.01	0.05	0.00	0.01	0.02	0.00
Cr_2O_3	0.04	0.04	0.00	0.00	0.06	0.00	0.00	0.06	0.00	0.05
FeO	2.32	2.13	2.21	1.77	1.91	2.20	1.94	2.15	1.44	1.70
MnO	0.09	0.12	0.09	0.12	0.00	0.03	0.00	0.08	0.03	0.07
MgO	55.89	56.69	55.94	56.01	55.25	54.21	55.73	55.85	54.52	55.35
CaO	0.05	0.04	0.05	0.03	0.05	0.03	0.01	0.03	0.09	0.01
Na_2O	0.02	0.02	0.00	0.02	0.00	0.00	0.00	0.03	0.00	0.04
K_2O	0.03	0.00	0.00	0.00	0.00	0.01	0.02	0.00	0.02	0.00
F	5.70	5.84	6.25	4.56	3.63	3.14	3.59	3.72	4.14	4.03
Total	99.22	99.65	99.54	99.80	98.98	97.12	99.72	99.90	96.76	98.03
O=F	2.40	2.46	2.63	1.92	1.53	1.32	1.51	1.57	1.74	1.70
Total	96.82	97.20	96.91	97.88	97.45	95.80	98.20	98.33	95.02	96.33
Cations on the basis of 18(O)										
Si	3.796	3.759	3.780	3.986	4.116	4.099	4.100	4.051	4.012	3.981
Ti	0.032	0.025	0.027	0.030	0.012	0.040	0.030	0.033	0.034	0.048
Al	0.001	0.000	0.001	0.000	0.001	0.006	0.000	0.002	0.002	0.000
Cr	0.004	0.003	0.000	0.000	0.005	0.000	0.000	0.005	0.000	0.004
Fe	0.212	0.194	0.202	0.160	0.174	0.204	0.175	0.194	0.134	0.156
Mn	0.009	0.011	0.008	0.011	0.000	0.002	0.000	0.007	0.002	0.006
Mg	9.119	9.210	9.092	9.013	8.935	8.935	8.949	8.978	9.029	9.068
Ca	0.006	0.004	0.006	0.004	0.006	0.004	0.001	0.003	0.011	0.001
Na	0.002	0.002	0.000	0.002	0.000	0.000	0.000	0.003	0.000	0.004
K	0.002	0.000	0.000	0.000	0.000	0.001	0.001	0.000	0.001	0.000
F	1.974	2.012	2.156	1.557	1.244	1.101	1.225	1.270	1.454	1.401
Total	13.183	13.209	13.115	13.205	13.247	13.308	13.257	13.277	13.226	13.268
MTi*	9.38	9.44	9.33	9.22	9.13	9.20	9.16	9.22	9.21	9.28
Xmg*100	97.73	97.94	97.83	98.26	98.09	97.77	98.08	97.88	98.54	98.30
MTi/Si	2.47	2.51	2.47	2.31	2.22	2.25	2.23	2.27	2.30	2.33
F/(F+OH)	0.98	0.98	1.07	0.78	0.62	0.56	0.62	0.64	0.73	0.71
OH*	0.05	0.04	-0.14	0.43	0.76	0.86	0.75	0.71	0.53	0.57

*MTi=Mg+Fe+Mn+Ti+Ca]
*calculated

amphibole. Retrograde amphibole after clinohumite or forsterite is tremolitic. Typically the amphiboles also have high fluorine conc entration (about 2 wt%).

Clinohumite (Table 10)

Clinohumite contains only small amounts of Ti (< 0.5%). Fluorine content of Ambasamudram clinohumite varies from 3 to 4 wt%. The F/(F+OH) values of the clinohumite are about 0.7 which is somewhat higher than the previously reported clinohumite (Fig. 9). Rice (1980) demonstrated that the increase in stoichiometric amount of (OH, F) in the humite series from clinohumite to norbergite is accompanied by an increase in the mole fraction of fluorine F/(F+OH).

Gaspar (1992) introduced a new mineralogical criteria to identify the humite group minerals using the ratio of total octahedral cations including Ti to Si. This (MTi/Si, MTi= Mg + Fe + Mn + Ti + Ca) is found to be 3.0, 2.5, 2.33 and 2.25 respectively for the minerals norbergite, chondrodite, humite and clinohumite respectively. The Ambasamudram samples gave an average MTi/Si value of 2.27 (ranging from 2.21 to 2.38). The range of the values shows a bimodal distribution (Fig. 10). This suggests to a possibility of intergrowth of humite within clinohumite. But, neither petrographic observations or XRD pattern points to such intergrowth (Satish-Kumar and Niimi, 1998). It is possible that very thin lamellae that could not be identified by normal optical observation might be present.

Carbonates

Calcite usually lacks exsolution textures in most of the samples except SK 21 1. It generally contains very little dolomite component, but some pure dolomite is present in sample SK 21 1 as a primary phase. Dolomite is present as relict phase or retrograde phase in the marbles.

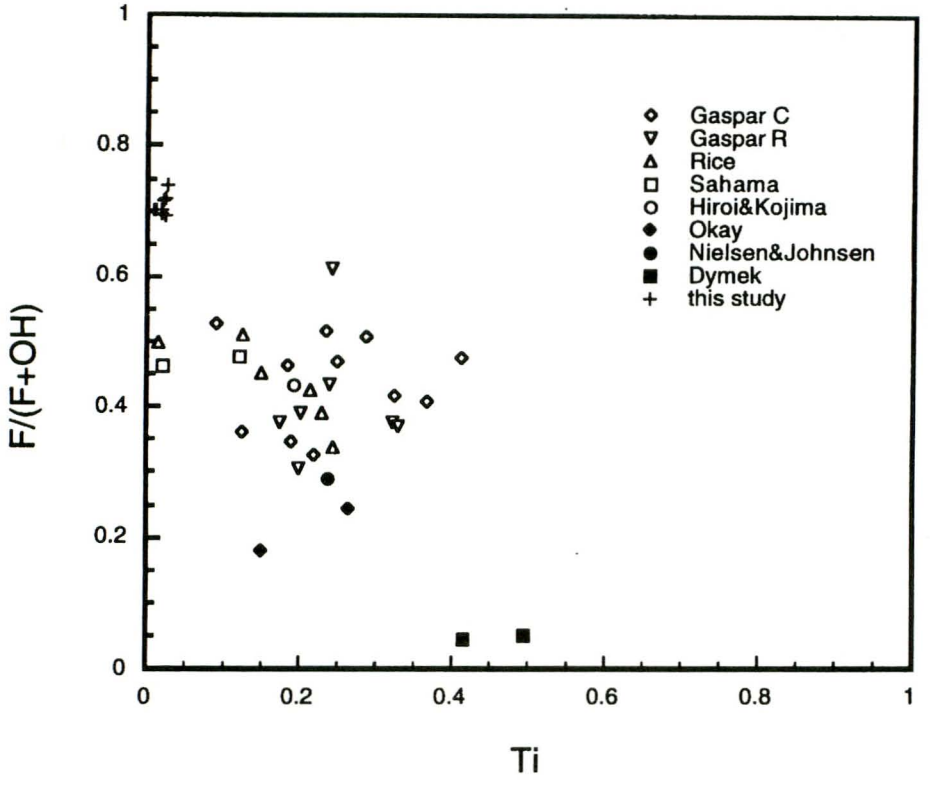

Fig. 9. F/(F+OH) versus titanium plot for clinohumites in carbonatites (Gaspar, 1992), in reaction rock (carbonatite with magnetite pyroxenite; Gaspar, 1992), in dolomitic limestone (Rice, 1980), in serpentinite (Dymek et al., 1988), in dolomitic marble (Hiroi and Kojima, 1988), in garnet pyroxenite (Okay, 1994), in plateau basalt (Nielsen and Johnson, 1978), in limestone (Sahama, 1953) and in marbles (after Satish-Kumar and Niimi, 1998).

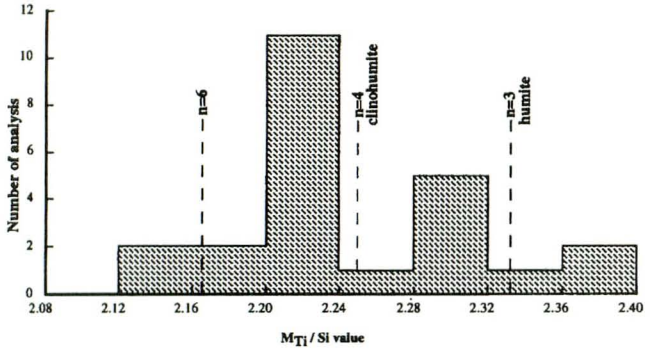

Fig. 10. Histogram representing the MTi/Si values of different analysis of clinohumite grains. Total 24 analyses of 8 clinohumite grains gave results indicative of clinohumite as the prominent phase (after Satish-Kumar and Niimi, 1998).

Partial petrogenetic grids in CASV system (Types-II & -III)

Partial petrogenetic grids of T-a_{CO_2}, P-a_{CO_2} and P-T were modeled using the computer program THERMOCALC v. 2.3 (Powell and Holland, 1988) with an updated thermodynamic dataset (Holland and Powell, 1990). Analyzed mineral chemical compositions were used in deriving the activities for the solid solution series. Activity-composition relations of grossular in garnet were modeled using the parameters of Engi and Wersin (1987) with the corrections, as noted in Harley and Buick (1992) and Fitzsimons and Harley (1994). Minor pyrope and spessartine components were treated as diluents. The activity composition relation of Oterdoom and Gunter (1983) were used for meionite and that of Aranovich and Podlesskii (1989) were used for anorthite activity in plagioclase. The activity composition data is presented in Table 11.

The reactions and textures observed in the calc-silicate rocks of Types II and III can be modeled in the CASV system, while recognizing that the involvement of clinopyroxene will affect mineral composition (e.g. garnet) and hence reaction stoichiometries in detail. Table 12 lists the univariant reactions for the different CASV assemblages. Two grid topologies were obtained, since the rocks were stabilized at P-T conditions close to the inversion between the grids, one with reactions involving [Mei], [Qtz] and [Grs] stable pseudo-invariant reactions for type-II and type-III assemblages, and the other with [Cal], [Wo] and [An] stable for the grossular-bearing marble assemblages.

The use of activity-corrected pseudo-petrogenetic grids require some explanation, as these reaction nets are strictly only valid for P-T or P-T-a_{CO_2} conditions close to the pseudo-invariants defined by buffering assemblages and the given component activities (Fitzsimons and Harley, 1994). As a consequence, such grids should not be used to trace out quan-

Table 11. Activity composition relations in TB calc-silicate rocks

Calc-silicate type	Mineral	Composition	Activity
II	Anorthite	X_{An}=0.94	0.94
II	Scapolite	EqAn=66	0.50
III	Granoblastic anorthite	X_{An}=0.98	0.98
III	retrograde anorthite	X_{An}=0.99	0.99
III	Granoblastic grossular	X_{Grs}=0.78	0.65
III	Grossular blebs	X_{Grs}=0.82	0.70
III	Scapolite in assemblage A	EqAn=85	0.79
III	Scapolite in aseemblage B	EqAn=76	0.55

Table 12. Calc-silicate reactions modelled in the $CaO-Al_2O_3-SiO_2-CO_2$ system.

calcite + quartz = wollastonite + CO_2	(An, Mei, Grs)*,**
3anorthite + calcite = meionite	(Wo, Qtz, Grs, V)*,**
grossular + quartz = 2wollastonite + anorthite	(Mei, Cal, V)*,**
Wollastonite + meionite = 2anorthite + grossular + $2CO_2$	(Cal, Qtz)*,**
3wollastonite + meionite +2calcite = 3grossular +$3CO_2$	(Wo, Qtz)*,**
wollastonite + anorthite + calcite = grossular + CO_2	(Mei, Qtz)*
meionite + quartz = wollastonite +3anorthite + CO_2	(Grs, Cal)*,**
anorthite + 2calcite + quartz = grossular + $2CO_2$	(Wo, Mei)*,**
meionite + 5wollastonite = 3grossular + 2quartz + CO_2	(An, Cal)**
meionite + 6wollastonite = 3Grossular + calcite + 3quartz	(An, V)**
meionite + 5calcite + 3quartz = 3grossular + $6CO_2$	(Wo, An)**
2meionite + quartz = grossular + 5anorthite +$2CO_2$	(Cal, Wo)**

* reactions stable in grids for Type-I and II assemblages only

** reactions stable in grids Type-IV assemblages only

*, ** reactions stable in both grids

titative P-T-a_{CO_2} evolutions without consideration of the changes in component activities that will occur as reaction progress and mineral compositions adjust to those changes in conditions. However, in the cases considered herein the activity-corrected approach will provide a close approximation to reality because a) the extent of the reaction of peak wollastonite-scapolite assemblages is small, and grossular production is correspondingly limited (i.e. in thin coronas); and b) reactions that involve pseudomorphic replacement (e.g. of scapolite) either progress 100% and replace whole grains, or progress 0% and leave individual grains intact. Thus, it is confident enough that initial scapolite compositions are preserved in the high-variance peak assemblage scapolite-wollastonite-clinopyroxene, and that the problems induced by the covariance of mineral compositions, as grossular forms, are largely avoided. Furthermore, as the initial assemblages involve plagioclase, which is near to pure anorthite in composition, the effects of T-dependent plagioclase-scapolite Ca-Na partitioning is minor in these rocks.

The reaction topologies developed for East Antarctic calc-silicates (see Harley and Buick, 1992 and Fitzsimons and Harley, 1994) are applicable to higher-pressure conditions (in the range of 7~9 kbar) where the assemblages, reactions and textures corresponds to the equilibria associated with [Wo], [An] and [Cal] pseudo invariant points. However, in the case of medium- to low-pressure assemblages the invariant points in these grids invert and, reactions about the pseudo-invariant points [Mei], [Grs] and [Qtz] become important (e.g. Fitzsimons and Harley, 1994). The peak metamorphic assemblages and the retrograde reactions seen at the Vellanad locality can be explained using the reactions discussed in the previous sections, which are focused on the [Mei] and [Qtz] points. The peak pressures assumed in our calculations are in the range of 5-6.5 kbar, and are derived from the geobarometry available from previous studies of the KKB (Santosh, 1987; Chacko et al., 1987).

Construction of partial petrogenetic grids in KCMASV system (Type-IV)

Prograde mineral reactions in the calcite-rich marble can be modeled in the system $K_2O-CaO-MgO-Al_2O_3-SiO_2-H_2O-CO_2$ (KCMAS) by mineral reactions in an impure dolomitic limestone. A fluid pressure of 6 kbar was used for the peak metamorphic assemblages and the end member mineral activities were used for solid solution series. There are some

inconsistencies in the computations of T-a_{CO_2} grids. The most important is that some minerals (phlogopite, clinohumite, pargasite, etc.) have high fluorine content in the system. These fluorine-rich phases show a granoblastic texture and are considered peak-metamorphic phases. Construction of phase diagrams should consider the fluorine content and experimental studies have indicated that with increasing fluorine content, the thermal stability of the hydrous phase considerably increases but the reaction topologies do not change (e.g. Osanai and Hensen, 1993). Consequently we adopt here the simple H_2O - CO_2 fluid system in order to signify the reaction topologies and constrain the minimum temperature of formation of such phases. Another important factor, which affects the topology, is the compositional variation of solid solution phases. The mineral composition varies widely in minerals between different layers such as amphiboles (tremolite to pargasite), phlogopite (phlogopite to Na-phlogopite) and spinel (with appreciable Fe content). It is found that the variation in topologies by using the activity corrections does not significantly affect much the slopes of the reactions. A third point to consider is that the system should be closed to the fluids. It was assumed that there was no fluid infiltration during peak metamorphic conditions while modeling the petrogenetic grids.

Peak metamorphic and fluid conditions

The type-I calc-silicate rocks are characterized by the assemblage of clinopyroxene + quartz + K-feldspar + scapolite + anorthite ± titanite ± calcite, which may have been produced from the metamorphism of a dolomitic precursor with some clay component. The equilibrium mineral assemblage (Cc + Qz + Sph + Cpx + Plg) is stable at a_{CO_2}>0.5 - 0.6 (outside the stability field of wollastonite).

Figure 11A is an isobaric T-a_{CO_2} partial petrogenetic grid calculated at 5kbar for the type-II assemblages (Satish-Kumar and Santosh, 1998). The absence of grossular in these calc-silicate rocks and the presence of coexisting wollastonite + anorthite, wollastonite + meionite, wollastonite + meionite + calcite etc. place constraints on the fluid characteristics of these calc-silicate rocks. At peak metamorphic temperatures of about 790°C the absence of grossular indicates the a_{CO_2} less than 0.59 (the [Grs] point).

Figure 12A is an isobaric T-a_{CO_2} grid calculated at 5 kbar, with mineral activities calculated for compositions corresponding to the Type-III granoblastic assemblages (Satish-Kumar and Harley, 1998). The pseudo-invariant points stable at 5 kb are [Qtz], [Mei] and [Grs], at temperatures of 760-835°C. The garnet-bearing assemblage A, containing peak wollastonite, scapolite, garnet and plagioclase, is stable at T > 835°C and would be stabilized relative to grossular-absent assemblages at moderate a_{CO_2} (< 0.48), if equilibrated in the presence of a fluid phase at such temperatures. This is also seen in the P-a_{CO_2} grid constructed for the peak temperatures (Fig. 12B). The key constraint on the minimum temperature of this assemblage is simply the breakdown of scapolite with

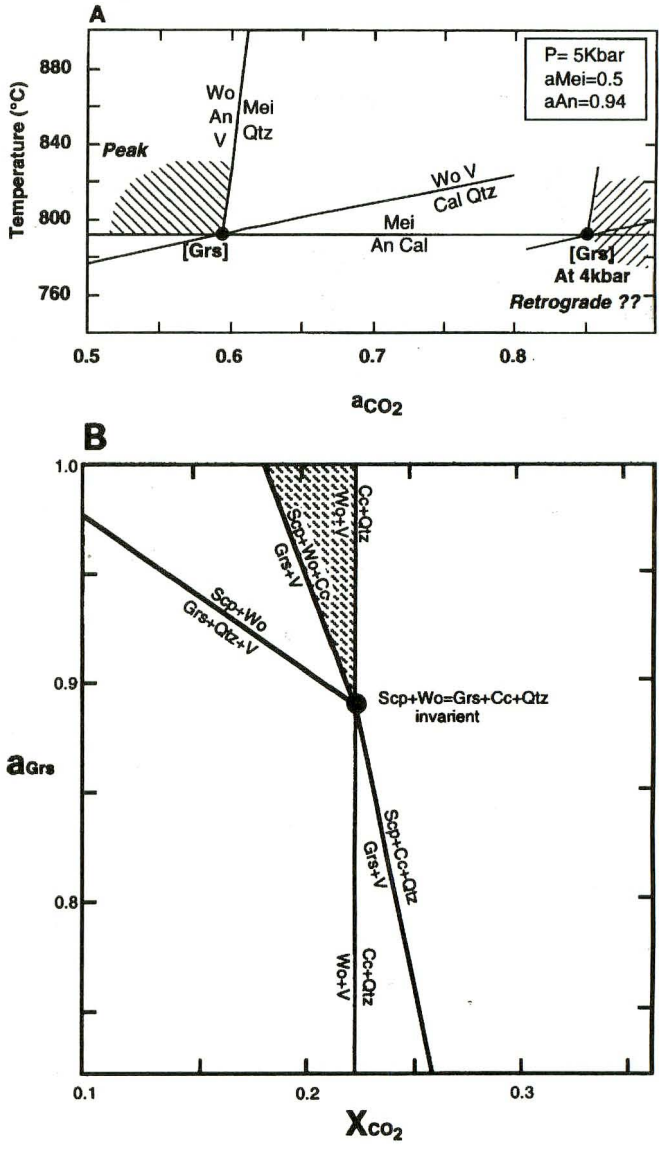

Fig. 11. (A) Isobaric T-a_{CO_2} reaction grid in the CASV system of the relevant mineral phases in Type-II retrograde calc-silicate assemblage. Notice the shift in the psuedoinvarient point [Grs] for a lower pressure condition of 4Kbar, where possibly the infiltration of carbonic rich fluids enhanced the retrograde reactions. Also notice the maximum a_{CO_2} of the peak assemblage can be constrained by the [Grs] psuedoinvarient point (after Satish-Kumar and Santosh, 1998. (B) a_{Grs}-X_{CO_2} diagram for Nuliyam assemblage (after Harley and Santosh, 1995). The hatched area represents the stability field of Nuliyam scapolite + wollastonite + calcite + vapour without the formation of grossular in the given P-T conditions. The absence of grossular in the assemblage can be used as a minimum estimate of a_{CO_2} for the peak assemblage.

aMei of 0.79, and the inferred temperature in Fig. 12A would be lower by some 50-70°C if the experimental data of Huckenholz and Seiberl (1990) were applied rather than the dataset of Holland and Powell (1990) and the corroborative experiments of Baker and Newton (1991). This minimum T is relatively independent of estimated P (Baker and Newton, 1991). Assemblage B, which is grossular-absent, also contains scapolite with lower EqAn, and hence lower aMei. This assemblage provides no further constraints on the T-a_{CO_2} conditions than those afforded by assemblage A.

The assemblage forsterite + diopside + K-feldspar + phlogopite + calcite + dolomite is stable at the invariant point marked I1 in the T-a_{CO_2} grid (Fig. 13A). The fluid composition in equilibrium with this assemblage is nearly pure CO_2, and the minimum temperature is about 700°C. The presence of high fluorine concentrations in phlogopite, amphibole and humites attest to a high temperature stability of amphibolite facies assemblages overlapping the granulite field. The equilibria involving the fluorine-rich phases will be shifting to higher temperatures by about 100-150°C (Valley et al., 1982;

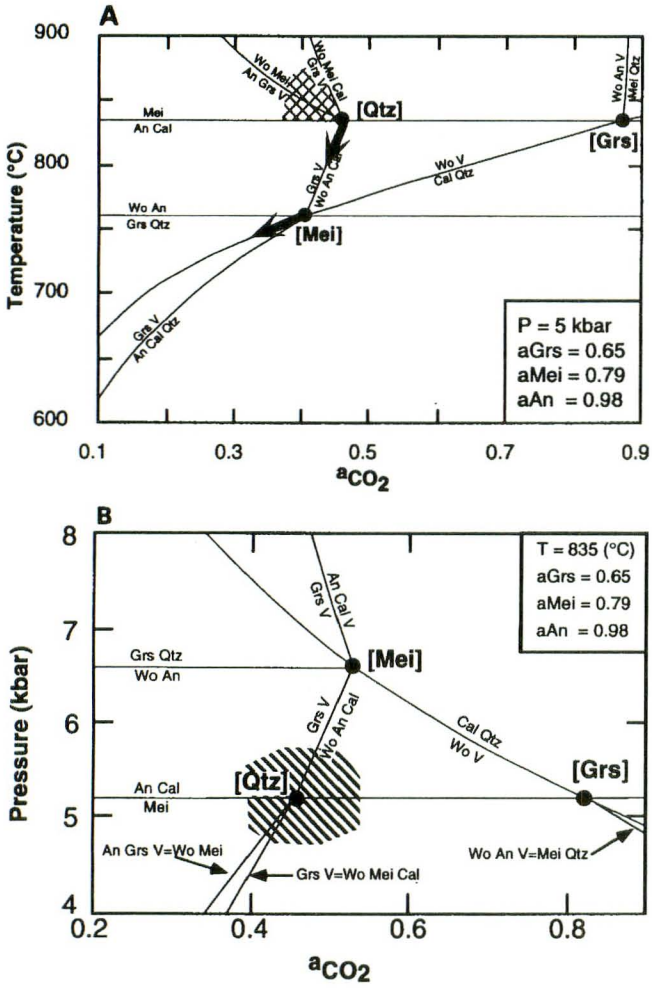

Fig. 12. (A) Isobaric T-a_{CO_2} grid for the type-III assemblages computed at 5 kbar. Mineral activities deduced from chemical analysis of individual mineral phases. The shaded portion including the [Qtz] pseudo invariant point indicates the peak metamorphic conditions. From the reaction textures observed it can be deduced that the type-II assemblages have a significant cooling component during the post peak path (after Satish-Kumar and Harley, 1998). (B) Isothermal P-a_{CO_2} grid for type-III assemblages constructed at 835°C. The shaded portion including the [Qtz] pseudo invariant point indicates the peak metamorphic conditions. From the reaction textures observed alternative to the initial cooling the texture can be "misinterpreted" to be resulting from compression, which is not the case with the KKB calc-silicate rocks (after Satish-Kumar and Harley, 1998).

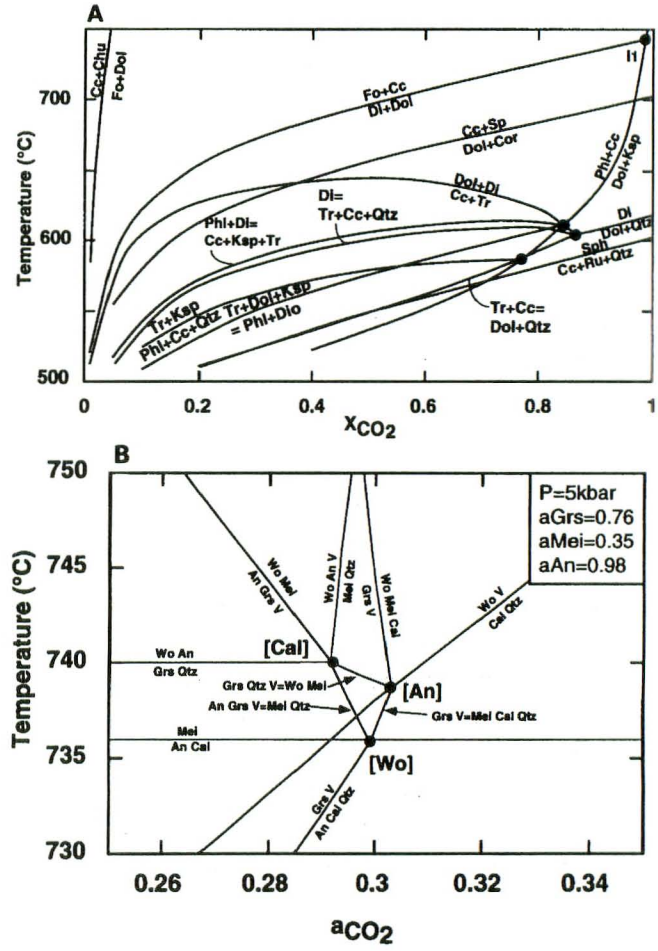

Fig. 13. (A) Isobaric T-a_{CO_2} reaction grid of the relevant mineral phases in type-IV dolomitic marbles, calculated at 5kbars and unit activities. A. Marble mineral paragenesis with mineral reactions showing the internal buffering within the layers. Mineral abbreviations are Cal- calcite; Chu-clinohumite; Dol-dolomite; Di-diopside; Fo-forsterite; Ksp-Kfeldspar; Phl-phlogopite; Qtz-quartz; Sp-spinel; Sph-titanite; Tr-tremolite. (B). Activity corrected T-a_{CO_2} grid for the grosssular-bearing assemblages in the type-IV dolomitic marbles. Notice the topology is entirely different from the other grids in the CASV system, with [An], [Wo], and [Cal] pseudo invariant points becoming stable instead of [Qtz], [Mei] and [Grs]. Even though there is not much variations in the P-T fluid conditions the grid topology has inverted because of the variation in mineral compositions.

Peterson et al., 1981). Pargasitic amphibole is also indicative of high temperature stability of the assemblages (Experimental reversal of 100 mole % pargasite occurred at 1075°C at 5 kbar; Oba 1980). The humite-bearing assemblages in some layers indicate a very low CO_2 fluid composition. Since $\delta^{18}O$ values of calcite grains co-existing with humite show no evidence for infiltration of water rich fluids, the fluid composition in equilibrium with this assemblage must have been internally buffered. The grossular-bearing assemblage indicates fluid-absent conditions or a low fluid activity during cooling from higher temperatures (Fig. 13B). Together these observations constitute important evidence for fluids with compositions controlled layer-by-layer.

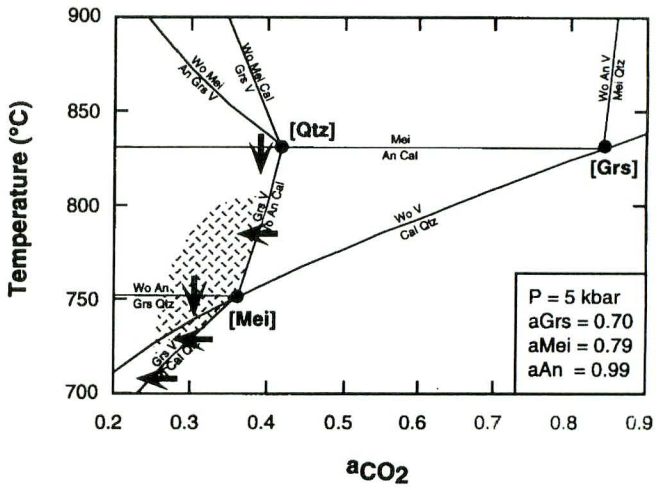

Fig. 14. An isobaric partial petrogenetic grid constructed in the CASV system at 5 kb using the reduced activities of garnet, scapolite and plagioclase of the retrograde assemblage in Type-III calc-silicate rocks (after Satish-Kumar and Harley, 1998). The arrow head indicates the cooling path based on the reaction textures observed.

Formation conditions of retrograde textures

In type-II calc-silicates the major reaction textures noticed are wollastonite break down, meionite break down and formation of scapolite-quartz symplectites. The meionite breakdown reaction is an indicator for cooling and is independent of vapor activity (Fig. 11A), whereas wollastonite breakdown and formation of meionite+quartz symplectites can be either due to compression, an increase in CO_2 activity of the system, or cooling at a_{CO_2} greater than the [Grs] point. These three reactions are typical in the type-II calc-silicate rocks. The extensive wollastonite breakdown to meionite-quartz symplectite can be explained by the external ingress of CO_2 rich fluids. This is evident from the shifting of the [Grs] point towards high a_{CO_2} with decreasing pressure (Fig. 11A). The absence of grossular formation reactions can also be used as a constraint for calculating fluid compositions (Fig. 11B), which approximates to about 0.2 (Harley and Santosh, 1995).

The conditions of formation of the various reaction textures described for Type-III calc-silicate rocks can be considered with reference to Figure 14, in an isobaric T-a_{CO_2} grid calculated at 5 kbar, with mineral component activities appropriate to the retrograde mineral assemblages (Satish-Kumar and Harley, 1998). Following equilibration near [Qtz], the sequence of reaction textures indicates that further garnet (GrsIII) either developed through cooling alone, or along a buffering reaction such as [Qtz] itself. The breakdown of scapolite is consistent with simple cooling (with or without any change in P) across the reaction (Grs, Qtz, Wo, V). Similarly, grossular - quartz coronas may have formed on cooling through ca. 750°C across the reaction (Mei, Cal, V). In both these cases there is no requirement for the influx or involvement of any fluid phase during the retrogression. In contrast, the development of grossular rinds between wollastonite and anorthite + calcite aggregates, formed through breakdown of previous scapolite, and of grossular blebs on anorthite, calcite and quartz, appears to require the infiltration of an externally-derived aqueous fluid, at temperatures of ca. 800-700°C. The latter textures are most likely to have been controlled by the respective reactions (Mei, Qtz) and (Mei, Wo), both of which have steep dT/da_{CO_2} and dP/dT slopes and also produce grossular along with vapor on their high-temperature sides. The effects of decreasing pressure on the positions of the vapor-bearing reactions depicted will generally translate them to lower a_{CO_2} for a given temperature (Fig. 14). Hence, cooling (and decompression) does not account for these textures, which are instead ascribed to the reaction of calc-silicates with low-a_{CO_2} fluids, perhaps derived from the crystallization of leucosome patches and veins in adjacent khondalites.

The retrograde reactions in Type-IV marbles suggest the role of CO_2 in reaction progress. The formation of scapolite-quartz and retrogression of forsterite and clinohumite are primary evidences for this. Scapolite-quartz symplectites are stable only at high a_{CO_2} conditions (Harley and Santosh, 1995). In humite-bearing assemblages, fluid composition shifted from low-a_{CO_2} during peak metamorphic conditions to higher a_{CO_2} during retrogression. But, most of the CO_2 will be consumed to form the products (see reactions R14 and R15). Neither chemographic relations nor carbon or oxygen isotope signatures ($\delta^{13}C$= 2.1‰ $\delta^{18}O$= 21‰, Satish-Kumar and Santosh, 1996a) permit the infiltration of aqueous fluid during retrogression. Because reactions observed in marbles mostly consume CO_2 they cannot proceed under low a_{CO_2}-conditions. This suggests that retrogression took place in the presence of externally derived carbonic fluids.

Fluorine enrichment-evidence for internal isochemical buffering

The origin of fluorine-rich clinohumite can be attributed to one of the two processes: 1) a metasomatic process resulting from the external influx of fluorinated fluids, 2) preferential internal partitioning. The former is normally the case in the contact aureoles, where granitic and granodioritic intrusion injects fluids to the impure limestone causing the formation of fluorine-rich clinohumite (e.g. Moore and Kerrick, 1976). Pradeepkumar et al. (1996), based on the geochemical studies of mineral and rock samples of Ambasamudram marbles, suggested an extraneous origin for the fluids, which they attributed to the granitic gneiss, which expelled aqueous fluorinated fluids. This contradicts with the results of the present study. The mineral chemical analyses show that clinohumite in Ambasamudrum marbles is fluorine rich. Rice (1980) described that it is possible that all marbles that contain fluorine rich clinohumite have not resulted from metasomatic introduction of fluorine and that concentration of fluorine can result from strong "partitioning" of fluorine into hydrous minerals. The primary evidence is from the stable isotopes of calcite in association with the clinohumite (Satish-Kumar and Santosh, 1996a). The lack of synmetamorphic granitic activity suggests an internal fluid buffering rather than external fluid influx. Calcite-rich marbles are usually impermeable to fluids, except for fracture controlled fluid infiltration (Holness and Graham, 1991; 1995). The clinohumite bearing assemblages at Ambasamudram are calcite-rich and hence supports our view that they were not affected by the external influx.

The origin of fluorine in the Ambasamudram clinohumites can be attributed to the isochemical reactions involving (OH-F) silicates such as amphiboles or phlogopite, which are abundant in the marble (Satish-Kumar and Niimi 1998). Fluorine distribution of humite > pargasite > phlogopite is clearly suggesting that fluorine has concentrated during progressive metamorphism. Rice (1980) attributed to the partitioning of fluorine into hydrous silicates relative to H_2O-CO_2 fluids. The source for the high concentration of fluorine in clinohumite can be attributed to this internal buffering mechanism of fluorine concentration.

Implications for Pressure-Temperature-Fluid evolution

Like calc-silicate rocks in other granulite terrains (cf., Warren et al., 1987; Hiroi et al., 1987; Harley and Buick, 1992; Harley et al., 1994; Fitzsimons and Harley, 1994), those in the KKB exhibit varied assemblages and textures. In particular, reaction textures involving grossular in calc-silicate rocks place important constraints on the retrograde P-T histories of granulites (Harley and Buick, 1992). For example, texture such as grossular rimming wollastonite with either anorthite or meionite is regarded as an index for cooling-dominated P-T paths, whereas those involving the breakdown of initial grossular denote a decompressional P-T path. Calc-

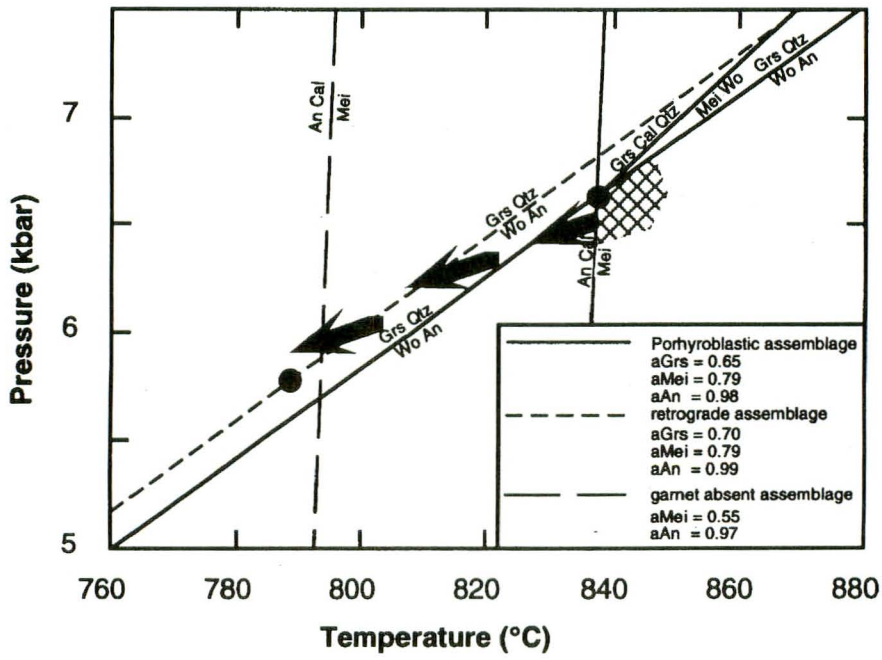

Fig. 15. P-T grid showing the vapour absent calc-silicate equilibria from the Kerala Khondalite Belt (after Satish-Kumar and Harley, 1998). The numerals inside squares are corresponding activities used in computation. The arrow head represents the post peak metamorphic evolution and is controlled by the formation of garnet+quartz corona as well as meionite (less EqAn) break down.

silicate mineral assemblages can be used only to define a broad view with regard to the peak metamorphic conditions. The KKB calc-silicates record peak metamorphic temperatures above 830°C based on the lower bound of meionite equilibria. Stability of scapolite + wollastonite with respect to grossular + calcite + quartz in these rocks provides an upper limit of pressure conditions to be 6.5 kbar at 830°C (Satish-Kumar and Harley, 1998). The [Qtz] absent assemblages in the calc-silicate stabilized around 830∞C and 5-5.5 kbar (Fig. 15). The meionite breakdown reaction in type-II calc-silicate rocks indicates that cooling proceeded below 790°C, accompanied by the formation of grossular-quartz coronas (Fig. 15).

The fluid conditions appeared to have varied between the different calc-silicate rocks and this controlled the peak metamorphic assemblages, especially between type-II and type-III rocks. Coexisting wollastonite - anorthite, calcite - anorthite - quartz, and calcite - anorthite - wollastonite, in the absence of grossular producing reactions, in type-II calc-silicate rocks, imply that the aco_2 was greater than 0.5 for typical granulite P-T conditions, whereas the occurrence of grossular-rich garnet in the type-III calc-silicate rocks (type-III) indicates that the aco_2 of any fluid in these rocks was lower than 0.45. In contrast to this internal buffering of fluid composition during the peak metamorphic conditions, there was localized influx of carbonic fluid on the retrograde P-T path which resulted in the formation of type-II reaction assemblages. This fluid influx occurred on the cooling path, that is independently constrained from metapelites, to have been accompanied by decompression.

Metamorphic evolution of the Trivandrum Block

Previous studies on the evaluation of the peak metamorphic conditions of the Trivandrum Block granulites suggest a temperature range from 700 to 800°C at a pressure range of 5 to 6 kbar (Harris et al., 1982; Srikantappa et al., 1985; Chacko et al., 1987; Santosh, 1987). Chacko et al. (1987) identified three major chronological events in the TB, viz. (1) migmatization (2) charnockite-forming event and (3) development of second generation of cordierite in khondalites during uplift. The P-T evolution corresponding to this attest to a clockwise path with decompressional uplift of the terrain. Santosh (1987) based on detailed textural analysis and fluid inclusion studies in cordierite bearing lithologies, also suggested an isothermal decompression for the terrain. The incipient charnockite formation regionally observed in the terrain have been attributed as a result of carbonic fluid influx (Santosh et al., 1991, 1990; Farquhar and Chacko, 1991)

Peak metamorphic conditions of TB revisited

Recently, Chacko et al. (1996) reevaluated the peak metamorphic conditions of the TB granulites. They suggested an ultra-high temperature metamorphism (840 to 1070°C; 8.5 to 9.6 kbar) for the terrain. A regional variation of temperatures, higher towards the massive charnockites on both northern and southern margins of the terrain has been considered as an evidence for heat input from charnockitic magma (Chacko et al., 1996).

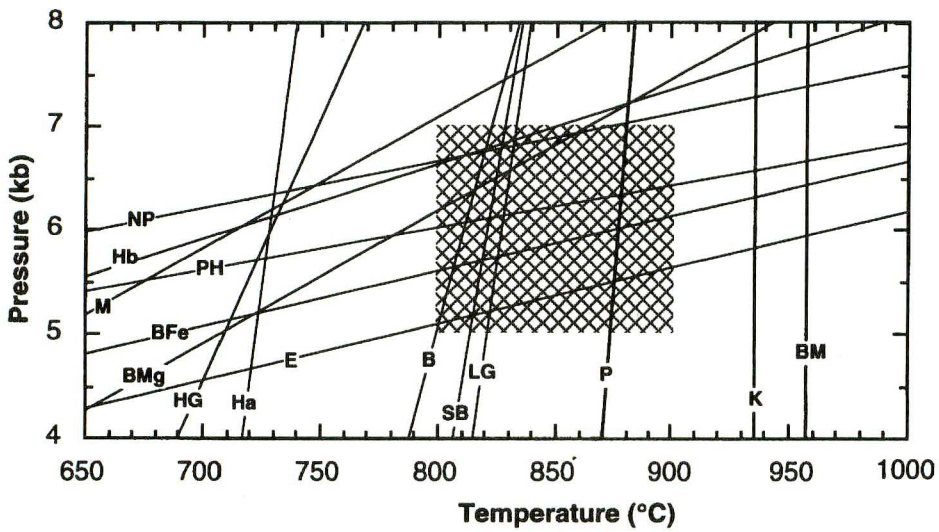

Fig. 16. Metamorphic temperature-pressure estimations in charnockites and pyroxene granulites from the Trivandrum Block. The cross hatched area represents the average peak metamorphic conditions. The solid lines are representative temperature and pressure estimates using different calibration from a single pair of garnet-orthopyroxene in sample SK 16 2 and clinopyroxene-orthopyroxene (Abbreviations are B: Bhattacharya et al., 1991 (BFe and BMg have similar reference to B); BM Bertrand and Mercier, 1985; E: Eckert et al., 1991; Ha and Hb are Harley, 1984; HG: Harley and Green, 1982; K: Kretz, 1982; LG: Lee and Ganguly, 1988; M: Moecher et al., 1988; P: Powell, 1978; PH: Powell and Holland, 1988)

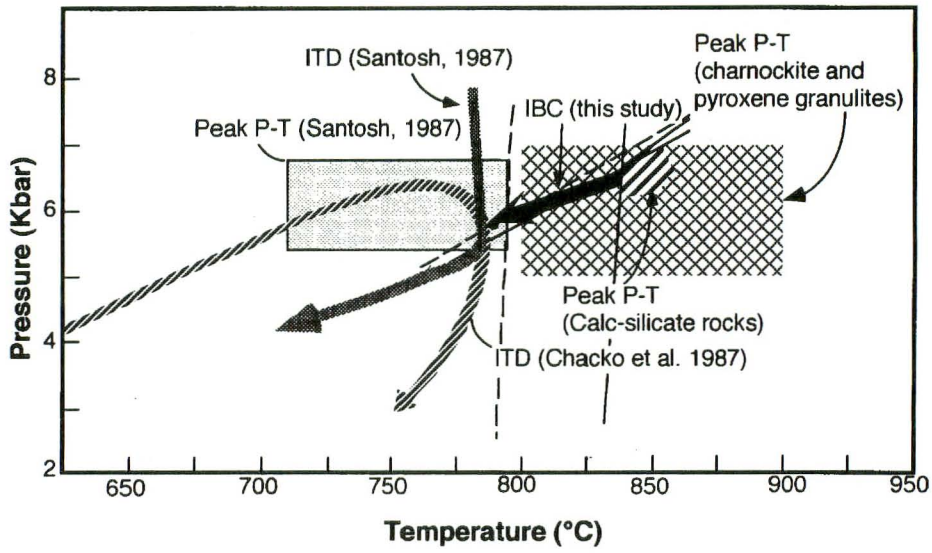

Fig. 17. P-T evolution of the KKB, compiled from data reported in this study (modified after Satish-Kumar and Harley, 1998) and the results of previous regional and local case studies of metapelites and garnet-orthopyroxene rocks (Santosh, 1987; Chacko et al., 1987). Note IBC deduced from the calc-silicates is interpreted to precede the ITD documented from fluid inclusions and metapelite textures. Thin lines represent calc-silicate equilibra.

Suites of charnockitic and pyroxene granulitic rocks that are exposed adjacent to the metacarbonate rocks were examined for peak metamorphic P-T estimation. A summary of the data is presented in Figure 16. Garnet-orthopyroxene geothermobarometer (Bhattacharya et al., 1991) and two-pyroxene thermometer (Kretz, 1982), both, gave temperature estimates mostly between 800 and 900°C with garnet-orthopyroxene-plagioclase-quartz barometer yielding pressures between 5 and 7 kbar at ambient temperatures. These results are consistent with the recent estimates of Chacko et al. (1996).

The reaction relations and topologies seen in the metacarbonate assemblages necessitate a re-evaluation of the metamorphic evolution of the TB. The fluid-absent equilibria related to the granoblastic quartz-absent assemblage indicate peak conditions of >837°C at < 6.6 kbar. The peak temperature defined here is significantly higher than those previously deduced from regional P-T studies of the KKB, which cluster at 725±50°C (Santosh, 1987; Chacko et al., 1987), but is consistent with new estimates from garnet-orthopyroxene and two-pyroxene granulites that occur in nearby localities (850±50°C and 6±1 kbar) and with recent estimates based on the Al-in orthopyroxene thermometer (ca. 850°C and 7 kbar, Chacko et al., 1996).

Recent studies of dehydration-melting processes in leptynitic gneisses at Manali, near Trivandrum and Vellanad (Braun et al., 1996) also point to metamorphic temperatures in excess of 800°C in this part of the KKB. Such relatively high peak-metamorphic temperatures could have been generated through thermal perturbation caused by intrusion of Nagarkovil massive charnockite into KKB gneisses, as proposed recently by Chacko et al. (1996). Similar observation can be made for the Madurai Block also where massive charnockites might have been the heat source for the high-temperature metamorphism.

A number of the reaction textures now preserved in the metacarbonates are consistent with post-peak cooling to 750°C whilst pressures were still >5 kbar. This near-isobaric P-T trajectory contrasts with the decompressional (ITD) P-T evolution documented from previous studies of the KKB (Santosh, 1987; Chacko et al., 1987: Santosh et al., 1990). However, as the previously deduced ITD evolution occurred at temperatures < 750°C (Santosh, 1987), the P-T record in the calc-silicates can be reconciled with that seen in the metapelites if the cooling textures pre-date the ITD cordierite-forming textures described in the earlier studies. In this scenario, the KKB P-T path would be one that initially involved near-isobaric cooling (IBC) at 5-6 kbar from peak conditions of > 837°C to ca. 750°C and subsequently involved continued cooling but with substantial exhumation, resulting in a final phase of post-peak decompression to 3-4 kbar at temperatures less than 750°C. Figure 17 shows this proposed two-stage post-peak evolution path (Satish-Kumar and Harley, 1998). The ITD phase of this post-peak evolution correlates with medium- to low-pressure fluid infiltration events including the post-peak reaction of hydrous fluids with the calc-silicate rocks, and the influx of carbonic fluids to produce incipient charnockite in the pelitic gneisses of the KKB (e.g. Santosh et al., 1991; Santosh and Wada, 1993; Harley and Santosh, 1995).

Fluid inclusion studies also provide good supporting evidences for the fluid evolution of the metacarbonate rocks (Satish-Kumar and Santosh, 1998). The formation of charnockites adjacent to the wollastonite calc-silicate rocks was the result of decompressional carbonic fluid influx, which had partially affected the calc-silicate rocks also. The movement of fluids might have taken place through mesoscopic fractures or alkaline dikes (Santosh and Wada, 1993; Farquhar and Chacko, 1991).

Alkaline magmas are potential carriers for carbonic fluids in granulite terrains. In a study of charnockite formation, Farquhar and Chacko (1991) have advocated that alkaline dikes expelled voluminous quantities of carbonic fluids to transform adjacent gneiss to charnockite. Similar observation can be also made at Nuliyam, where flanks of an alkaline pegmatite are charnockitized. When regionally observed, it can be noticed that the charnockitization phenomena becomes more pronounced from the central KKB south toward the Nagarkovil massif. Even though it is a premature suggestion, it is likely that the charnockitic magmas have supplied the carbonic fluids to the KKB from the deep crustal reservoirs, and caused the wide spread fluid-induced charnockite formation.

In summary, this study provides evidence for a high-temperature peak metamorphism in TB, with an initial isobaric cooling, before the terrain was uplifted (Fig. 17). The fluid conditions were internally buffered during prograde and peak metamorphic conditions and local external fluid influx at different sectors of decompression. Among the late stage fluid influx, the most significant one is of the terrain wide post-peak metamorphic syn-charnockitic-carbonic fluid infiltration.

Acknowledgments

The present work forms a part of the Ph.D. thesis submitted to the Osaka City University. The author wishes to express his gratitude to the Ministry of Education, Science, Culture and Sports, Japan (MONBUSHO) for financial assistance during the doctoral course and JSPS postdoctoral fellowship during which this work was completed. My sincere thanks to Profs. M. Yoshida, M. Santosh, H. Wada, and S. L. Harley, for constant encouragements. I wish to thank Drs. S. Yoshikura, S.L Harley, Y. Motoyoshi T. Okudaira and Y. Yoshino for helping me with EPMA analyses at various occasions. Dr. S. Dasgupta is thanked for the constructive comments. A part of the expenses for the present study was defrayed from the Grant-in-Aid for the International Scientific Research, and that for the General Scientific Research, of MONBUSHO, project No. 08041109 and No. 08454160 respectively, both of which were led by M. Yoshida of Osaka City University. This paper is a contribution to IGCP-368 and the Gondwana Research Group.

References

Aranovich, L.Ya. and Podlesskii K.K. 1989. Geobarometry of high-grade metapelites: simultaneously operating reactions. In: Evolution of Metamorphic Belts J.S. Daly, R.A. Cliff, and B.W.D. Yardley, (eds.) *Geological Society Special Publication*, **43**, 45-62.

Baker, J. and Newton, R.C. 1991. A re-re-determination of the reaction 3 anorthite + calcite = meionite. *Geological Society of America Abstracts with Programs* 1991, 23. A52.

Bartlett, J.M., Harris, N.B.W., Hawksworth, C.J. and Santosh, M. 1995. New isotope constraints on the crustal evolution of South India and Pan-African granulite metamorphism. In: India and Antarctica during the Precambrian, M. Yoshida, and M. Santosh, (eds.) *Geological Society of India, Memoir*-**34**, 391-397.

Bartlett, J.M. 1995. *Crustal evolution of the high-grade terrain of South India*. Unpub. Ph.D. thesis, Open University, U.K., 230p.

Bhattacharya, A., Krishnakumar, K.R., Raith, M. and Sen, S.K. 1991. An improved set of a-X parameters for Fe-Mg-Ca garnets and refinements of the orthopyroxene-garnet thermometer and the orthopyroxene-garnet-plagioclase-quartz barometer. *Journal of Petrology*. **32**, 629-656.

Beckinsale, R.D., Revees-Smith, G., Gale, N.H., Holt, R.W. and Thompson, B. 1982. Rb-Sr and Pb-Pb whole rock isochron ages and REE data for Archaean gneisses and granites, Karnataka State, South India. In: *Indo-Us Workshop on Precambrian of South India* (abstr.) National Geophysical Research Institute, Hyderabad, 35-36.

Bence, A.E. and Albee, A.L. 1968. Empirical correlation factors for electron microanalysis of silicates and oxides. *Journal of Geology*, **76**, 382-403.

Bernard-Griffiths, J., Jahn, B.M. and Sen, S.K. 1987. Sm-Nd isotopes and REE geochemistry of Madras granulites: an introductory statement. *Precambrian Research*, **37**, 343-355.

Bertrand, P. and Mercier, J.-C. 1985. The mutual solubility of coexisting ortho- and clinopyroxene: toward an absolute geothermometer for the natural system? *Earth and planetary Science Letters*, **76**, 109-122.

Brandon, A.D. and Meen, K. 1995. Nd isotopic evidence for the position of southernmost Indian terranes within East Gondwana. *Precambrian Research*, **70**, 269-280.

Braun, I., Raith, M. and Ravindra Kumar, G.R. 1996. Dehydration-melting phenomena in leptynitic gneisses and the

generation of leucogranites: a case study from the Kerala Khondalite Belt, southern India. *Journal of Petrology*, **37**, 1285-1305.

Chacko, T., Ravindra Kumar, G.R. and Newton, R.C. 1987. Metamorphic P-T conditions of the Kerala (South India) Khondalite belt, A granulite facies supracrustal terrain. *Journal of Geology*, **95**, 343-358.

Chacko, T., Lamb, M. and Farquhar, J. 1996. Ultra high temperature metamorphism in the Kerala Khondalite Belt. In: The Archaean and Proterozoic terrains in Southern India within East Gondwana M. Santosh and M. Yoshida (eds.) *Gondwana Research Group Memoir*-**3**, 157-165.

Chadwick, B., Vasudev, V.N. and Ahmed, N. 1996. The Sandur schist belt and its adjacent plutonic rocks-implications for late Archaean crustal evolution in Karnataka. *Journal of Geological Society of India*, **47**, 37-57.

Choudhary, A.K., Harris, N.B.W., van Calsteren, P. and Hawksworth, C.J. 1992. Pan-African charnockite formation in Kerala, south India. *Geological Magazine*, **129**, 257-64.

Dasgupta S. 1993. Contrasting mineral paragenesis in high temperature calc-silicate granulites: examples from the Eastern Ghats. *Journal of Metamorphic Geology*, **11**, 193-202.

Drury, S.A. and Holt, R.W. 1980. The tectonic framework of the south Indian craton: a reconnaissance involving LANDSAT imagery. *Tectonophysics*, **65**, 1-15

Drury, S.A., Harris, N.B.W., Holt, R.W., Reeves-Smith, G.W. and Wrightman, 1984. Precambrian tectonics and crustal evolution in South India. *Journal of Geology*, **92**, 1-20.

Dymek, R.F., Boak, J.L. and Brothers, S.C. 1988. Titanian chondrodite- and titanian clinohumite-bearing metadunite from 3800 Ma Isua supracrustal belt, West Greenland: Chemistry, Petrology, and Origin. *American Mineralogist*, **73**, 547-558.

Eckert, J.O., Newton, R.C. and Kleppa, O.J. 1991. The DH of the reaction and recalibration of garnet-pyroxene-plagioclase-quartz geobarometers in the CMAS system by solution calorimetry. *American Mineralogist*, **76**, 148-160.

Engi, M. and Wersin, P. 1987. Derivation and application of a solid solution model for calcic garnet. *Schweizerisches Mineralogisches und Petrographisches Mitteilungen.*, **67**, 53-73.

Evans, B.W., Shaw, D.M. and Houghton, D.R. 1969. Scapolite stoichiometry. *Contributions to Mineralogy and Petrology*, **24**, 293-305.

Farquhar, J. and Chacko, T. 1991. Isotopic evidence for involvement of CO_2-bearing magmas in granulite formation. *Nature*, **354**, 60-63.

Fitzsimons, I.C.W. and Harley, S.L. 1994. Garnet coronas in scapolite -wollastonite calc-silicates from East Antarctica: the application and limitations of activity-corrected grids. *Journal of Metamorphic Geology*, **12**, 761-777.

Gasper, J.C. 1992. Titanian clinohumite in the carbonatites of the Jacupianga Complex, Brazil: Mineral chemistry and comparisons with titanian clinohumite from other environments. *American Mineralogist*, **77**, 168-178.

Glassley, W.E. 1983. Deep crustal carbonates as CO_2 fluid sources: evidence from metasomatic reaction zones. *Contributions to Mineralogy and Petrology*, **84**, 15-24.

Hansen, E.C., Newton, R.C., Janardhan, A.S., and Lindenberg, S. 1995. Differentiation of late Archaean crust in the Eastern Dharwar craton, Krishnagiri-Salem area, South India. *Journal of Geology*, **103**, 629-651.

Hansen, E.C., Janardhan, A.S., Newton, R.C., Prame, W.K.B.M. and Ravindrakumar G.R. 1987. Arrested charnockite formation in southern India and Sri Lanka. Contributions to Mineralogy and Petrology, 96, 225-244.

Harley, S.L. 1984. The solubility of alumina in orthopyroxene coexisting with garnet in FeO-MgO-Al_2O_3-SiO_2 and CaO-FeO-MgO-Al_2O_3-SiO_2. *Journal of Petrology*, **25**, 665-696.

Harley, S.L. and Buick, I.S. 1992. Wollastonite-Scapolite Assemblages as indicators of granulite pressure-temperature-fluid histories: The Rauer Group, East Antarctica. *Journal of Petrology*, **33**, 693-728.

Harley, S.L. and Green, D.H. 1982. Garnet-orthopyroxene barometry for granulites and peridotites, *Nature* **300**. 697-701.

Harley, S.L. and Santosh, M. 1995. Wollastonite at Nuliyam, Kerala, southern India: a reassessment of CO_2-infiltration and charnockite formation at a classic locality. *Contributions to Mineralogy and Petrology*, **120**, 83-94.

Harley, S.L., Fitzsimons, I.C.W. and Buick, I.S., 1994. Reactions and textures in wollastonite-scapolite granulites and their significance for pressure-temperature-fluid histories of high-grade terranes. *Precambrian Research*, **66**, 309-323.

Harris, N.B.W. and Bickle, M.J. 1989. Advective fluid transport during charnockite formation; an example from southern India. *Earth and Planetary Science Letters* **93**, 151-156.

Harris, N.B.W., Jackson, D.H., Mattey, D.P., Santosh, M. and Bartlet, J. 1993. Carbon-isotope constraints on fluid advection during contrasting examples of incipient charnockite formation. *Journal of Metamorphic Geology*, **11**, 833-843.

Harris, N.B.W., Holt, R.W. and Drury, S.A. 1982. Geobarometry, geothermometry, and late Archean geotherms from granulite facies terrain of South India. *Journal of Geology*, **90**, 509-527.

Harris, N.B.W., Santosh, M. and Taylor, P.N. 1994. Crustal

evolution in South India: Constraints from Nd. isotopes. *Journal of Geology*, **102**, 139-150.

Harris, N.B.W., Bartlett, J.M. and Santosh, M. 1996. Neodymium isotope constraints on the tectonic evolution of East Gondwana. *Journal of Southeast Asian Earth Science*, **14**, 119-125.

Hiroi, Y. and Kojima, H. 1988. Petrology of dolomitic marbles from Kasumi rock, Prince Olav coast, east Antarctica. *Proceedings of the Symposium on Antarctic Geoscience, National Institute of Polar Research*, **2**, 96-109.

Hiroi, Y., Shiraishi, K., Motoyoshi, Y. and Katsushima, T. 1987. Progressive metamorphism of calc-silicate rocks from the prince Olav and Soya Coasts, East Antarctica. *Proceedings of the Symposium on Antarctic Geoscience, National Institute of Polar Research*, **1**, 73-97.

Holland, T.J.B. and Powell, R. 1990. An enlarged and updated internally consistent thermodynamic dataset with uncertainties and correlations: the system K2O-Na2O-CaO-MgO-MnO-FeO-Fe2O3-Al2O3-TiO2-SiO2-C-H2-O2. *Journal of Metamorphic Geology*, **8**, 89-124.

Holness, M.B. and Graham, C.M. 1991. Equilibrium dihedral angles in the system H2O-CO2-NaCl-calcite, and implications for fluid flow during metamorphism. *Contributions to Mineralogy and Petrology*, **108**, 368-383

Holness, M.B. and Graham, C.M. 1995. P-T-X effects on equilibrium carbonate-H2O-CO2-NaCl dihedral angles: constraints on carbonate permeability and the role of deformation during fluid infiltration. *Contributions to Mineralogy and Petrology*, **119**, 301-313.

Huckenholz, H.G. and Seiberl, W.M. 1990. Stability and phase reactions of carbonate-scapolite solid solutions under the P-T regime of the deeper crust. *Terra Abstracts*, **2**. 81.

Jackson, D.H. and Santosh, M. 1992. Dehydration reaction and isotope front transport induced by CO_2 infiltration at Nuliyam, South India. *Journal of Metamorphic Geology*, **10**, 365-382.

Janardhan, A. S., Newton, R. C. and Hansen, E. C. 1982. The transformation of amphibolite gneiss to charnockite in southern Karnataka and northern Tamilnadu. *Contributions to Mineralogy and Petrology*, **79**, 130-149.

Jayananda, M., Janardhan, A.S., Sivasubramaniam, P. and Peucat, J.J. 1995. Geochronologic and isotopic constraints on granulite formation in the Kodaikkanal area, Southern India. In: India and Antarctica during the Precambrian, M. Yoshida and M. Santosh, (eds.) *Geological Society of India, Memoir*-**34**, 373-390.

Kretz, R. 1982. Transfer and exchange equilibria in a portion of the pyroxene quadrilateral as deduced from natural and experimental data. *Geochimica et Cosmochimica Acta*, **46**, 411-421.

Kretz, R. 1983. Symbols for rock-forming minerals. *American Mineralogist*, **68**, 277-279

Krishnanath, R. 1981. Coexisting Humite-Chondrodite-spinel-Magnesian Calcite assemblage from the calc-silicate rocks of Ambasamudram, Tamilnadu, India. *Journal of Geological Society of India*, **22**, 235-242.

Lee, H.Y. and Ganguly, J. 1988. Equilibrium compositions of coexisting orthopyroxene and garnet: experimental determinations in the system FeO-MgO-Al_2O_3-SiO_2, and applications. *Journal of Petrology*, **29**, 93-113.

Miller, J.S., Santosh, M., Pressley, R.A., Clements, A.S. and Rogers, J.J.W. 1996. A Pan-African thermal event in southern India. *Journal of Southeast Asian Earth Sciences* **14**, 127-136.

Moecher, D.P. and Essene, E.J. 1991. Calculation of CO_2 activities using scapolite equilibria: constraints on the presence and composition of a fluid phase during high grade metamorphism. *Contributions to Mineralogy and Petrology*, **108**, 219-240.

Moecher, D.P., Essene, E.J. and Anovitz, L.M. 1988. Calculation and application of clinopyroxene-garnet-plagioclase-quartz geobarometers. *Contributions to Mineralogy and Petrology*, **100**, 92-106.

Moore, J.N. and Kerrick, D.M. 1976. Equilibria in siliceous dolomites of the Alta aureole, Utah. *American Journal of Science*, **276**, 502-524.

Motoyoshi Y., Thost D.E. and Hensen B.J. 1991. Reaction textures in calc-silicate granulites from the Bolingen Islands, Prydz Bay, East Antarctica: implications for the retrograde P-T path. *Journal of Metamorphic Geology*, **9**, 293-300.

Nielsen, T.F.D. and Johnsen, O. 1978. Titaniferous clinohumite from Gardiner Plateau complex, East Greenland. *Mineralogical Magazine*, **42**, 99-102.

Oba, T. 1990. Experimental study on the tremolite-pargasite join at variable temperatures under 10 kbar. *Proceedings of the Indian Accademy of Sciences*, **99**, 81-90.

Okay, A.I. 1994. Sapphirine and Ti-clinohumite in ultra-high-pressure garnet-pyroxene and eclogite from Dabie Shan, China. *Contributions to Mineralogy and Petrology*, **116**, 145-155.

Oterdoom, W.H. and Gunter, W.D. 1983. Activity models for plagioclase and CO_2-scapolite-An analysis of field and laboratory data. *American Journal of Science*, **283-A**, 255-282.

Petersen, E.U., Essene, E.J., Peacor, D.R. and Valley, J.W. 1982. Fluorine end-member micas and amphiboles. *American Mineralogist*, **67**, 538-544.

Peucat, J.J., Vidal, P., Bernard-Griffiths, J. and Condie, K.C. 1989. Sr. Nd. and Pb. isotopic systematics in the Archean

low- to high-grade transition zone in southern India: syn-accretion vs post accretion granulites. *Journal of Geology*, **97**, 537-550.

Powell, R. 1978. The thermodynamics of pyroxene geotherms. *Philosophical Transactions, Royal Society of London*, series A, **288**, 457-469.

Powell, R. and Holland, T.J.B. 1988. An internally consistent dataset with uncertainties and correlations: 3. Applications to geobarometry, worked examples and a computer program. *Journal of Metamorphic Geology*, **9**, 173-204.

Pradeepkumar, A.P. and Krishnanath, R. 1996. Rare earth element mobility in halogenated aqueous fluids in the humite-marbles of Ambasamudram, Kerala Khondalite Belt, India. *Current Science*, **70**, 1066-1074.

Radhika, U.P., Santosh, M. and Wada, H. 1995. Graphite occurrences in Southern Kerala: Characteristics and genesis. *Journal of Geological Society of India*, **45**, 653-666.

Raith, M., Karmakar, S. and Brown, M. 1997. Ultra-high-temperature metamorphism and multistage decompressional evolution of sapphirine granulites from the Palni Hill ranges, southern India. *Journal of Metamorphic Geology*, **15**, 379-399.

Rajesh, H.M., Santosh, M. and Yoshida, M. 1996. The felsic magamatic province in East Gondwana: implications for Pan-African tectonics. *Journal of Southeast Asian Earth Sciences*, **14**, 275-292.

Ravindrakumar, G.R. and Venkatesh Raghavan, 1992. The incipient charnockites of transition zone, granulite zone and khondalite zone of South India: Contrasting mechanisms and controlling factors. *Journal of Geological Society of India*, **39**, 293-302.

Rice, J.M. 1980. Phase equilibria involving humite minerals in impure dolomitic limestones, Part I. Calculated stability of clinohumite. *Contributions to Mineralogy and Petrology*, **71**, 219-235.

Rogers, J.J.W. 1986. The Dharwar craton and the assembly of peninsular India. Journal of Geology, 94, 129-144.

Rogers, J.J.W. and Mauldin, L.C. 1994. A review of the terrains of southern India. In: Subbarao, K.V. (ed.) *Volcanism*. Wiley Eastern Ltd., 157-171.

Sacks, P.E., Nambiar, C.G. and Walters, L.J. 1997. Dextral Pan-African shear along the southwestern edge of the Achankovil shear belt, South India: Constraints on Gondwana reconstructions. *Journal of Geology*, **105**, 275-284.

Sahama, Th.G. 1953. Minerology of the humite group. *Ann. Accad. Sci. Fennicae, III. Geology and Geography*, **31**, 1-50.

Santosh, M. 1987. Cordierite gneisses of Southern Kerala, India: petrology, fluid inclusions and implications for crustal uplift history. *Contributions to Mineralogy and Petrology*, **96**, 343-356.

Santosh, M. 1996. The Trivandrum and Nagarkovil granulite blocks. In: The Archaean and Proterozoic terrains in Southern India within East Gondwana. M. Santosh and M. Yoshida (eds.) *Gondwana Research Group Memoir-3*, 243-279.

Santosh, M. and Drury, S.A. 1988. Alkali granites with Pan-African affinities from Kerala, South India. *Journal of Geology*, **96**, 616-626.

Santosh, M. and Wada, H. 1993. A carbon isotope study of graphites from the Kerala Khondalite belt, Southern India: Evidence for CO_2 infiltration in granulites. *Journal of Geology*, **101**, 643-651.

Santosh, M., Iyer, S.S., Vasconcellos, M.B.A. and Enzweiler, J. 1989. Late Precambrian alkaline plutons in southwest India: geochronologic and rare earth element constraints on Pan-African magmatism. *Lithos*, **24**, 65-79.

Santosh, M., Harris, N.B.W., Jackson, D.H. and Mattey, D.P. 1990. Dehydration and incipient charnockite formation: A phase equilibria and fluid inclusion study from South India. *Journal of Geology*, **98**, 915- 926.

Santosh, M., Jackson, D.H. and Harris, N.B.W. 1993. The significance of channel and fluid inclusion CO_2 in cordierite: Evidence from carbon isotopes. *Journal of Petrology*, **34**, 233-258.

Santosh, M., Jackson, D.H., Harris, N.B.W. and Mattey, D.P. 1991. Carbonic fluid inclusions in South Indian granulites: evidence for entrapment during charnockite formation. *Contributions to Mineralogy and Petrology*, **108**, 318-330.

Santosh, M., Kagami, H., Yoshida, M. and Nanda-Kumar, V. 1992. Pan-African charnockite formation in East Gondwana: geochronologic Sm-Nd and Rb-Sr and petrogenetic constraints. *Bulletin Indian Geologists Association*, **25**, 1-10.

Satish-Kumar, M. and Santosh, M. 1996a. Calc-silicate rocks and marbles from the Kerala Khondalite Belt: An appraisal. In: *The Archaean and Proterozoic terrains in Southern India within East Gondwana*. M. Santosh and M. Yoshida (eds.) *Gondwana Research Group Memoir-3*, 279-316.

Satish-Kumar, M. and Santosh, M. 1996b. Wollastonite-bearing calc-silicate rocks adjacent to charnockites at Nuliyam, Trivandrum Block, southern India. (Field guide stop-6) In: *The Archaean and Proterozoic terrains in Southern India within East Gondwana*. M. Santosh and M. Yoshida (eds.) *Gondwana Research Group Memoir-3*, 357-364.

Satish-Kumar, M. and Santosh, M. 1996c. The calc-silicate rocks and marbles of Ambasamudram, southern Tamil Nadu, South India. (Field guide stops - 9 & 10) In: *The*

Archaean and Proterozoic terrains in Southern India within East Gondwana. M. Santosh and M. Yoshida (eds.) *Gondwana Research Group Memoir*-**3**, 377-384.

Satish-Kumar and Harley, S.L. 1998. Reaction textures in scapolite-wollastonite-grossular calc-silicate rock from the Kerala Khondalite Belt, southern India: evidence for high temperature metamorphism and initial cooling. *Lithos*, **44**, 83-99.

Satish-Kumar, M. and Santosh, M. 1998. A petrologic and fluid Inclusion study of calc-Silicate - charnockite associations from southern Kerala, India: Implications for CO_2 Influx. *Geological Magazine*, **135**, 27-45.

Satish-Kumar, M. and Niimi, N. 1998. Fluorine rich clinohumites from Ambasamudram, southern India: Mineralogic and FTIR spectroscopic characterization. *Mineralogical Magazine*, **62**, 509-519.

Satish-Kumar, M., Santosh, M. and Yoshida, M. 1995. Wollastonite from calc-silicates of the Kerala Khondalite Belt, southern India: Changing fluid regimes during deep crustal metamorphism. *Current Science*, **68**, 813-819.

Satish-Kumar, M., Santosh, M. Harley, S.L. and Yoshida, M. 1996. Calc-silicate assemblages from the Kerala Khondalite Belt, southern India: Implications for pressure-temperature-fluid histories. *Journal Southeast Asian Earth Science*, **14**, 245-263.

Shaw, D.M. 1960. The geochemistry of scapolite: Part-I, previous work and general mineralogy. *Journal of Petrology*, **1**, 218-260.

Srikantapa, C., Raith, M. and Spiering, B. 1985. Progressive charnockitization of a leptynite-khondalite suite in southern Kerala, India: evidence for formation of charnockites through decrease in fluid pressure. *Journal of Geological Society of India*, **26**, 849-872.

Srikantappa, C., Raith, M., and Touret, J.L.R. 1992. Synmetamorphic high-density carbonic fluids in the lower crust: Evidence from the Nilgiri granulites, southern India. *Journal of Petrology*, **33**, 733-760.

Taylor, P.N., Chadwick, B., Moorbath, S., Ramakrishnan, M. and Viswanatha, M.N. 1984. Petrography, chemistry, and isotopic ages of Peninsular Gneiss, Dharwar acid volcanic rocks and the Chitradurga granite with special reference to the late Archaean evolution of the Karnataka craton, southern India. *Precambrian Research*, **3**, 349-375.

Touret, J.L.R. and Hansteen, T.H. 1988. Geothermometry and fluid inclusions in a rock from the Doddabeta charnockite complex, southwest India. *Rendoconti della Societa Italiana di Mineralogia Petrologia*, **43**, 65-82.

Uniikrishnan Warrier, C., Santosh, M. and Yoshida, M. 1995. First report of Pan-African Sm-Nd and Rb-Sr mineral isochron ages from regional charnockites of southern India. *Geological Magazine*, **132**, 253-260.

Valley, J.W., Petersen, E.U., Essene, E.J., and Bowman, J.R. 1982. Fluorphlogopite and fluortremolite in Adirondack marbles and calculated C-O-H-F fluid compositions. *American Mineralogist*, **67**, 545-557.

Warren, R.G., Hensen, B.J. and Ryburn, R.J., 1987. Wollastonite and scapolite in Precambrian calc-silicate granulites from Australia and Antarctica. *Journal of Metamorphic Geology*, **5**, 213-223.

Manuscript received November 20, 1998.
Revised manuscript accepted March 19, 1999.